

AD-A136 874

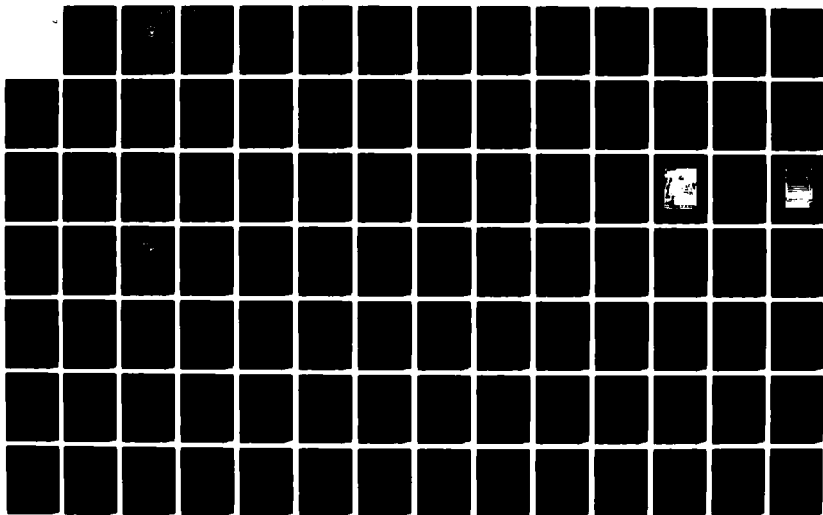
FLOW GENERATION IN A NOVEL CENTRIFUGAL DIFFUSER TEST  
DEVICE(U) NAVAL POSTGRADUATE SCHOOL MONTEREY CA  
P VIDOS SEP 83

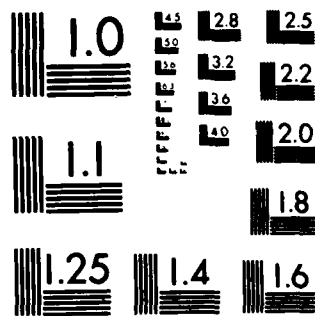
1/2

UNCLASSIFIED

F/G 20/4

NL





MICROCOPY RESOLUTION TEST CHART  
NATIONAL BUREAU OF STANDARDS-1963 A

AD A 136874

# NAVAL POSTGRADUATE SCHOOL

Monterey, California



DTIC  
ELECTE  
JAN 17 1984

## THESIS

S D

FLOW GENERATION IN A NOVEL  
CENTRIFUGAL DIFFUSER TEST DEVICE

by

Panagiotis Vidos

September 1983

Thesis Advisor:

R. Shreeve

Approved for public release; distribution unlimited.

DTIC FILE COPY

84 01 16 018

UNCLASSIFIED

SECURITY CLASSIFICATION OF THIS PAGE (When Data Entered)

REPORT DOCUMENTATION PAGE		READ INSTRUCTIONS BEFORE COMPLETING FORM
1. REPORT NUMBER	2. GOVT ACCESSION NO. AD-A136874	3. RECIPIENT'S CATALOG NUMBER
4. TITLE (and Subtitle) Flow Generation in a Novel Centrifugal Diffuser Test Device		5. TYPE OF REPORT & PERIOD COVERED Master's Thesis; September 1983
		6. PERFORMING ORG. REPORT NUMBER
7. AUTHOR(s) Panagiotis Vidos		8. CONTRACT OR GRANT NUMBER(s)
9. PERFORMING ORGANIZATION NAME AND ADDRESS Naval Postgraduate School Monterey, California 93943		10. PROGRAM ELEMENT, PROJECT, TASK AREA & WORK UNIT NUMBERS
11. CONTROLLING OFFICE NAME AND ADDRESS Naval Postgraduate School Monterey, California 93943		12. REPORT DATE September 1983
		13. NUMBER OF PAGES 104
14. MONITORING AGENCY NAME & ADDRESS (if different from Controlling Office)		15. SECURITY CLASS. (of this report) Unclassified
		15a. DECLASSIFICATION/DOWNGRADING SCHEDULE
16. DISTRIBUTION STATEMENT (of this Report)  Approved for public release; distribution unlimited.		
17. DISTRIBUTION STATEMENT (of the abstract entered in Block 20, if different from Report)		
18. SUPPLEMENTARY NOTES		
19. KEY WORDS (Continue on reverse side if necessary and identify by block number)  Centrifugal Diffuser Test Device CDTD Preliminary		
20. ABSTRACT (Continue on reverse side if necessary and identify by block number) Recognition of the need to develop optimum diffusers for advanced centrifugal compressors, resulted in the design and manufacture of a novel low speed test facility for centrifugal diffuser testing. The CDTD was designed to allow the flow angle and wall boundary profiles into the test diffuser to be controlled by variable geometry in the flow generator. The present study reports on the design		

DD FORM 1 JAN 73 1473

EDITION OF 1 NOV 65 IS OBSOLETE  
S/N 6102-LF-014-6601

1

UNCLASSIFIED

SECURITY CLASSIFICATION OF THIS PAGE (When Data Entered)

UNCLASSIFIED

SECURITY CLASSIFICATION OF THIS PAGE (When Data Entered)

## 20. ABSTRACT (Continued)

of the flow generator and the analysis of the internal flow using a NASA computer code (MERIDL). First test results are given and are compared with the results of a control volume analysis. The flow angle control technique was found to work effectively but to give somewhat smaller angles (by  $4^\circ$ ) than were predicted. It was concluded that the information obtained would allow scaling of the device, however an analysis code was needed which would accept the real physical boundary conditions.

Accession For	
NTIS GRA&I	<input checked="checked" type="checkbox"/>
DTIC TAB	<input type="checkbox"/>
Unannounced	<input type="checkbox"/>
Justification	
By	
Distribution/	
Availability Codes	
Dist	Avail and/or Special
A/1	



S. N 0102- LF-014-6601

UNCLASSIFIED

SECURITY CLASSIFICATION OF THIS PAGE (When Data Entered)

Approved for public release; distribution unlimited.

Flow Generation in a Novel  
Centrifugal Diffuser Test Device

by

Panagiotis Vidos  
Captain, Hellenic Air Force  
B.S., Hellenic Air Force Academy, 1972

Submitted in partial fulfillment of the  
requirements for the degree of

MASTER OF SCIENCE IN AERONAUTICAL ENGINEERING

from the

NAVAL POSTGRADUATE SCHOOL

September 1983

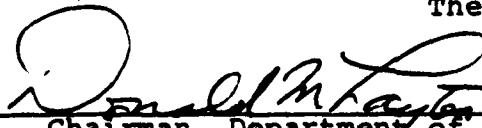
Author:



Approved by:



Thesis Advisor



Chairman, Department of Aeronautics



Dean of Science and Engineering

# ABSTRACT

➤ Recognition of the need to develop optimum diffusers for advanced centrifugal compressors, resulted in the design and manufacture of a novel low-speed test facility for centrifugal diffuser testing. The CDTD was designed to allow the flow angle and wall boundary profiles into the test diffuser to be controlled by variable geometry in the flow generator. The present study reports on the design of the flow generator and the analysis of the internal flow using a NASA computer code (MERIDL). First test results are given and are compared with the results of a control volume analysis. The flow angle control technique was found to work effectively but to give somewhat smaller angles (by  $4\frac{1}{2}^\circ$ ) than were predicted. It was concluded that the information obtained would allow scaling of the device; however, an analysis code was needed which would accept the real physical boundary conditions. ⚡

## TABLE OF CONTENTS

I.	INTRODUCTION -----	11
II.	CDTD DESIGN -----	14
	A. DESCRIPTION -----	14
	B. DESIGN CALCULATIONS -----	16
	C. FLOW ANALYSIS -----	16
	1. Flowfield Modeling -----	18
	2. Results -----	18
III.	PRELIMINARY TEST PROGRAM -----	20
	A. INSTRUMENTATION -----	20
	1. Installed for Preliminary Measurements --	20
	2. Not Installed for Preliminary Measurements -----	21
	B. PROGRAM OF MEASUREMENTS -----	21
	C. RESULTS -----	22
IV.	DISCUSSION -----	23
	A. EXPERIMENTAL RESULTS -----	23
	B. THEORY AND EXPERIMENT -----	25
V.	CONCLUSIONS -----	27
	APPENDIX A: CDTD DESIGN CALCULATIONS -----	68
	APPENDIX B: FLOW MODELING CALCULATIONS FOR MERIDL INPUT -----	72
	APPENDIX C: CALCULATION OF THE MASS AVERAGED FLOW ANGLE -----	75
	APPENDIX D: CONTROL VOLUME ANALYSIS -----	79



APPENDIX E: MERIDL INPUT FILES -----	91
APPENDIX F: MERIDL OUTPUT FILES -----	95
LIST OF REFERENCES -----	103
INITIAL DISTRIBUTION LIST -----	104

### LIST OF SYMBOLS AND ABBREVIATIONS

A	Cross sectional area for hydraulic diameter calculation
$A_{JW}$	Total outflow area of one jet-wall ( $A_{JW} = .059 \text{ FT}^2$ )
$A_{SV}$	Outflow cross sectional area of one SV ( $A_{SV} = .000436 \text{ FT}^2$ )
$A_{T1}$	Total flow area out of the GC
$A_{T2}$	Total flow area out of the diffuser
$A_{MIX}$	Total mixing area per swirl vane
$A_i$	Area at station (i)
CTDD	Centrifugal diffuser test device
C	Wetted perimeter for hydraulic diameter calculation
$C_F$	Friction coefficient
$C_P$	Pressure term (sudden expansion)
$C_T$	Friction term
$d_h$	Hydraulic diameter
$\vec{F}$	Force
GC	Generating cylinder
IW	Total surface area of the inner walls of the CTDD
JW	Jet walls
$K_{b1}$	Blockage factor at the outlet of the swirl vanes
$K_{b2}$	Blockage factor at the inlet of the test section
$l$	Spanwise length (variable of integration)
$L_1$	Half exposed length of the generating cylinder ( $2L_1 = l_1$ )
$l_1$	Exposed length of the generating cylinder (total jet-wall spacing)

$L_2$	Half span of the test section ( $2L_2 = l_2$ )
$L_2^*$	Initially designed half span of the test section ( $2L_2^* = l_2^*$ )
$l_2$	Span of the test section
$l_2^*$	Initially designed span of the test section
$\dot{m}_i$	Mass flow rate
$M_{aw}$	Moment exerted on the wall surfaces by the air about the longitudinal axis of the CDTD
$N$	Number of corrugations per exposed length of the generating cylinder ( $N = 19.104 \text{ FT}^{-1}$ )
$\hat{n}$	Outward normal unit vector
OC	Outer casing of the CDTD
$P_{KIEL}$	Kiel probe
$P_{5H}$	Five hole probe
$P_{SGC}$	Static pressure at the surface of the generating cylinder
$P_{SOC}$	Static pressure at the surface of the outer casing
$P_{t1}$	Stagnation pressure at the outlet of the swirl vanes
$P'_{t1}$	Stagnation pressure after jet mixing
$P_w$	Normal stress on the non cylindrical surfaces of the swirl vanes
$P_1$	Static pressure at the outlet of a swirl vane
$\bar{R}$	Mean radius of the generating cylinder location ( $\bar{R} = 19.1 \text{ IN}$ )
$R_H$	Radius at the hub of the flow model
$R_h$	Hydraulic radius
$R_S$	Radius at the shroud of the flow model
$Re$	Reynolds number
$R_1$	Radius at the surface of the generating cylinder
$R_2$	Radius at the test section inlet

SV	Swirl vanes
TS	Test section
$\hat{t}$	Tangential unit vector
$V_z$	Axial velocity (at the z direction)
$V_{R_i}$	Radial velocity component at station (i)
$V_i$	Total velocity at station (i)
$\bar{V}_{IW}$	Average velocity for the flow over the inner walls of the CDTD
$\bar{V}_{ij}$	Area average velocity
$\bar{\bar{V}}_{ij}$	Mass average velocity
$V_{\theta i}$	Tangential velocity component at station (i)
$\bar{V}_1$	Average velocity out of the swirl vanes
Z	Number of corrugations per revolution of the generating cylinder
z	Longitudinal (axial) direction
$\beta_i$	Flow angle at station (i)
$\bar{\bar{\beta}}_2$	Mass average flow angle at the test section
$\nu$	Kinematic viscosity
$\rho_i$	Density at station (i)
$\psi$	Stream function

#### ACKNOWLEDGMENTS

The author would like to pay tribute to the inspiration and influence of Professor J.R. Erwin in the initiation and early phases of this study. Professor Erwin was the Naval Air Systems Command Visiting Research Professor in Aeronautics at the time of his passing on May 1st 1983. For the advice and association as professor and student, and for the personal association with his family, I express my gratitude.

## I. INTRODUCTION

Centrifugal compressors are currently used in gas turbine power units for turboprop aircraft, helicopters and auxiliary power production. The capability of achieving high pressure ratios per stage (12:1), and the simplicity of design & fabrication, are reasons for using centrifugal rather than axial stages in smaller engine types. The main disadvantage is the progressively lower efficiencies obtained as the pressure ratio is increased.

A major contributor to centrifugal compressor inefficiency is the performance of the diffuser which closely follows the impeller of the compressor. The purpose of the centrifugal diffuser is to convert most of the kinetic energy of the flow entering the diffuser vanes into static pressure, with the highest efficiency attainable.

The design of centrifugal diffusers is presently based mainly on experimental results for two dimensional and conical diffusers. While numerical methods are currently under development, computer solutions to viscous, three dimensional, unsteady, transonic flows, with adverse static pressure gradients are not yet available as verified tools to be used to optimize designs.

Centrifugal diffusers are currently tested only as components of high speed compressors or gas turbine engines.

This approach is very expensive and does not yield detailed, accurate information which is necessary to confirm design systems or to provide the basis for improved theoretical analysis.

A new test facility [Ref. 1] has been proposed and built, the so-called CDTD (Centrifugal Diffuser Test Device), which has as its main purpose the large scale, controlled simulation of the time-averaged inlet flow to centrifugal compressor diffusers. The device will allow the detailed evaluation of proposed diffuser geometries at an acceptable expense, and will permit validation of new computer analysis codes for diffusers operating in a fully subsonic flow regime.

This report deals only with the flow generation within the CDTD, the control of which was to be effected in a novel way. The flow was supplied through a central, swirl generating cylinder (GC) and the average angle of the flow into the diffuser under test, was to be controlled by covering or exposing more or less of the cylinder's length.

The design and the calculations on which the device was based, are given in Chapter II. In the same section are also described the results obtained of modeling the flow-field generation using the NASA computer code MERIDL [Ref. 2]. In order to use the code, in its standard form, artificial boundary conditions were used to obtain nearly representative conditions at the physical boundaries.

Selected results from the initial program of measurements, carried out on the CDTD, operating in effect without a diffuser, are given in Chapter III.

The flow angle control principle, was shown to work qualitatively, however the angle produced for a given exposed length of the central cylinder, were found to be less (by  $5^{\circ}$ - $10^{\circ}$ ) than were predicted in the design calculations.

Reasons for the observed differences between design and test results are discussed in Chapter IV. It is shown (Appendix D) that a control-volume analysis of the flow generation, in which the geometry of the swirl generating cylinder surface, mixing and wall effects are included, can be used to predict the measured results.

It is concluded in Chapter V that by using the results of measurements to establish reasonable values for unknown factors in the control-volume analysis, a means of scaling the design is obtained.

Finally, it is recommended that an axi-symmetric, inviscid analysis of the flow generation, in which the physical boundary conditions are more properly represented, be carried out.



## II. CTDD DESIGN

### A. DESCRIPTION

The Centrifugal Diffuser Test Device (CTDD), is located in the Cascade Building (213) at the Turbopropulsion Laboratory complex of the Naval Postgraduate School. A view of the apparatus is shown in Fig. 1. A schematic is shown in Fig. 2.

The philosophy in the design of the CTDD was to provide a nearly tangentially-directed, uniform airflow from a large cylinder, have a minimum decrease in tangential velocity between the cylinder and the test diffuser (conserving angular momentum) while the exposed length of the cylinder would control the radial component of velocity and hence the average flow angle ( $\beta_2$ ) entering the test diffuser.

The device consists of the following major components with their corresponding functions.

#### 1. Perforated Cylinder (Fig. 2, Index 5)

The perforated cylinder serves as a major structural component of the CTDD, holds the north and south plates in parallel and concentric alignment and provides uniformly distributed air at low velocity around its periphery.

#### 2. Generating Cylinder (Fig. 2, Index 10)

The generating cylinder is placed around the perforated cylinder and consists of the following components.

a. Central Section (Fig. 2, Index 12)

The central section is made of sets of small nozzles (not 2-D vanes as shown in the schematic) formed by pressing & bending sheet metal strips and soldering them to form a drum. A view of the complete section is shown in Fig. 3. The nozzles provide an almost tangential velocity which is controlled by the pressure supplied at the inlet.

b. North & South End Cylinders (Fig. 2, Index 11)

These support the central section. They each contain a short length of porous section inside of which cylindrical throttles (Fig. 2, Index 6) are arranged to slide. The throttles, operating separately, expose or cover the porous sections, so controlling the air supplied to the jet walls.

3. Jet Walls (Fig. 2, Index 3)

These are annular end walls containing nozzles distributed radially, so that nearly tangential injection is produced through them (the same nozzles as for the generating cylinder are used). By-pass air, depending on the throttle positioning is routed through the jet walls, to effect changes in the velocity distribution at the diffuser inlet. The jet walls are also the means for controlling the main airflow into the test section (TS). The mass flow through the swirl vanes, is controlled by moving the jet walls axially, and so exposing more or less of the swirl vane area. Thus the velocity profile and the average flow

angle ( $\beta_2$ ) at the test section, are controlled by the jet walls and associated throttle positions.

#### 4. Other Components

The outer casing (Fig. 2, Index 9) contains a contraction contour (Fig. 2, Index 8), which is designed to turn the flow into a radial, parallel-wall test section containing the diffuser vanes under test.

### B. DESIGN CALCULATIONS

The CDTD design calculations are presented in Appendix

A. The concepts of continuity and conservation of angular momentum were applied to an incompressible, inviscid flow. The detailed geometry of the inlet surface and effects of friction were not considered.

Selected flow angles ( $\beta_2$ ) and jet wall spacings ( $L_2$ ), were input into the derived formulae, and the results are given in Table A1 and Figure 29.

### C. FLOW ANALYSIS

A FORTRAN computer program MERIDL [Ref. 2] was used to obtain a prediction of the flowfield generated by the CDTD.

Specifically, in the design phase the main interest was to investigate the velocity behavior along the contraction contour (Fig. 2, Index 8), in order to verify that the flow is turned without adverse deceleration ahead of the test vanes, into the diffuser.

MERIDL, besides its general applications for calculating flows through blade rows in turbomachines, can obtain solutions for flow in annular ducts without blades.

The flow must be essentially subsonic and the solution obtained is for two-dimensional axi-symmetric, compressible, shock free flow. Upstream and downstream flow conditions can vary from hub to shroud, and provision is made for an appropriate correction for loss of stagnation pressure.

The analysis consists of the solution of the simultaneous, non-linear, finite-difference equations for the stream function ( $\psi$ ).

The following assumptions are made:

- (1) The fluid is a perfect gas with constant specific heat  $C_p$ .
- (2) The only forces along a hub-shroud orthogonal mesh line are those due to momentum and pressure gradient (viscous forces are neglected in that direction).
- (3) There is no heat transfer.
- (4) The upstream and downstream boundaries of the solution region are orthogonal to the streamlines.
- (5) The stream function is zero at the hub and 1.0 at the shroud.

The program generates an orthogonal mesh in the space between the hub and the shroud, by dividing it into equal increments along several hub-shroud lines. Spline curves are fit through the resulting points to obtain the streamwise

orthogonals. The normal orthogonals are obtained by a predictor-corrector technique. The solution of the equations follows an iterative method with successive overrelaxation.

### 1. Flowfield Modelling

An equivalent flowfield to the one generated by the CDTD had to be formulated in order to overcome MERIDL's inability to accommodate the real physical boundary condition along the generating cylinder.

The author of Reference 2 was consulted and the geometric model shown in Fig. 4 was developed after appropriate calculations were carried out (Appendix B).

The inflow stream was introduced with a constant whirl ( $R_{\theta}r = \text{const.}$ ) far upstream of the TS. The channel height was doubled so that the streamlines, close to the region of the contraction contour, approximated the actual flow pattern generated by the device .

The input files to MERIDL (Appendix E) were generated and the program was run using the Naval Postgraduate School's IBM 370-3033 computer.

### 2. Results

Selected tabulated results (for  $\psi = 0.0$  and  $\psi = 1.0$ ) from the converged output files generated by MERIDL are given in Appendix F.

The TEKTRONIX 618 plotter was used to plot the streamlines of the computed flowfield (Fig. 5a). An enlargement of the area of main interest around the contraction contour is shown in Fig. 5b.

The relative velocity along the outer casing wall ( $\psi = 1.0$ ), for the selected runs, is shown plotted in Fig. 6. The flow appears to be accelerating in the region of the contraction contour (stations 14-23) and then begins to diffuse.

Finally in Figures 7 and 8 the velocity and the flow angle variations are shown plotted for the  $\psi = 0.0$  streamline from the surface of the GC ( $R_1 = 1.5833$  FT) up to the TS inlet ( $R_2 = 2.1$  FT). The velocity is seen to diffuse smoothly and the flow angle decreases to almost a constant value at the inlet station to the test vanes.

A check was made of the velocity and flow angle uniformity at the location of the GC. The results are given in Table 1. Values between stations were obtained by linear interpolation of the tabulated output from MERIDL. The results show that the conditions expected, at the surface of uniform velocity and angle, appear to have been achieved with a maximum deviation of .5% in the velocity and 2.4% in the flow angle ( $\beta_1$ ) at outlet flow angles from  $60^\circ$  to  $75^\circ$ .

Comparisons of the predictions with measurements will be made when pressure taps have been installed along the outer casing and the contraction contour, as discussed in subsection III.A.2.

### III. PRELIMINARY TEST PROGRAM

Preliminary measurements were carried out as shown in Figure 9, using a short vaneless diffuser, obtained by replacing the plexiglass walls (Fig. 2, Index 13), with locally fabricated plywood walls (Fig. 9, Index 4). The walls ended at the intended location of the leading edge of the test vanes.

The data were taken using two pressure probes, one United Sensor 5-hole and one Kiel probe. Both probes were connected to a manometer board, inclined at a 30° angle for greater sensitivity.

#### A. INSTRUMENTATION

##### 1. Installed for Preliminary Measurements

The instrumentation arrangement is indicated in Figure 9. The 5-hole probe (Fig. 9, Index 1) was attached to the south half of the outer casing which could rotate to facilitate circumferential measurements. The radial position of the probe corresponded to the leading edge of the test vanes ( $R_2 = 25"$ ). The probe could traverse axially in order to obtain data for the total pressure and flow angle distributions, as well as for the velocity profile, produced across the outlet from the plywood walls (parallel to the main axis of the device).

The Kiel probe (Fig. 9, Index 5) was moved radially from the GC surface ( $R_1 = 19"$ ), up to the intended location of the LE of the test vanes ( $R_2 = 25"$ ), and axially (from wall to wall). The purpose of measurements inside the flow generator was specifically to obtain:

- a. The flow mixing pattern out of the swirl vanes and from the GC up to the outer casing.
- b. Wake visualization close to the surface of the GC.
- c. The blockage factor ( $K_{B_1}$ ) for the flow, at the exit of the nozzles.

## 2. Not Installed for Preliminary Measurements

A set of pressure taps was designed to be drilled on the contraction contour and on the outer casing, as shown in Figures 10a and 10b in order to obtain data to compare with the results generated using MERIDL.

The proposed arrangement is shown in Fig. 10a, drawn on the north (fixed) part of the apparatus. The circumferential tap distribution is indicated in Fig. 10b, for both rotating and fixed walls.

A tap size of .04 inches diameter (.001 m) was selected. Pressure data can be recorded using the laboratory's HP 3052 Data Acquisition System with Scanivalve interface.

## B. PROGRAM OF MEASUREMENTS

The goals of the preliminary measurements were:

- a. To verify the effectiveness of the flow control method,



- b. To visualize the flowfield,
- c. To verify circumferential symmetry,
- d. To measure the total pressure and flow angle ( $\beta_2$ ) distributions at the inlet to the test section.

A series of tests were conducted, at a plywood wall spacing of 2.62" (varying slightly circumferentially), at selected jet wall spacings and throttle settings. Probe measurements were also taken at various circumferential positions.

### C. RESULTS

Data from selected runs are presented in Tables 2 through 17.

The data obtained from the measurements were reduced using the methods of averaging derived in Appendix C. The averages were obtained assuming incompressible flow and using the equations for conservation of mass and angular momentum.

A computer program was developed, to carry out the required calculations. Spanwise (gapwise) integrations were accomplished using the subroutine DATINT from Reference 3.

From the computations, blockage factors ( $K_{b_2}$ ), and mass averaged flow angles ( $\bar{\beta}_2$ ) were obtained at the inlet of the test section for various configurations of the apparatus.

#### IV. DISCUSSION

##### A. EXPERIMENTAL RESULTS

The initial results showed that:

1. The flow control method was working, but the flow angle was not affected as much as was expected by jet wall spacing changes.
2. The measured maximum average flow angle  $\beta_2$  was less than the design angle of  $70^\circ$ .
3. The flowfield generated by the device was qualitatively as expected and mixing of the jets from the swirl vanes occurred very quickly.
4. Circumferential symmetry of the measured flow angle  $\beta_2$  at the exit of the plywood walls was not achieved.

In trying to explain the results, the importance of the leak which was forced to occur at the interface of the GC surface and the jet walls, in all but the maximum ( $l_1 = 24.375''$ ), spacings was examined. Table 2-9 gives data for  $l_1 = 24.375''$ .

A survey with a tuft at minimum jet wall spacing ( $l_1 = 7.0''$ ) showed that significant axial component of velocity and a vortex flow were generated at the gap, as shown in Figure IV.1 below.

A vortical recirculation region was established near the jet wall, between the outer casing (higher static pressure region) and the generating cylinder surface (lower

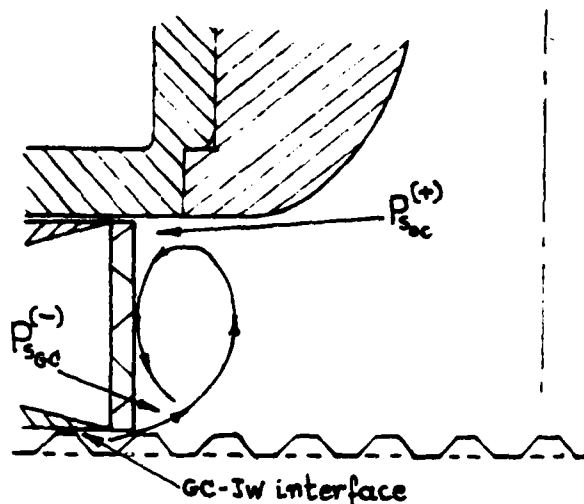


Figure IV.1. Schematic of the Vortex Flow Generated at the GC-JW Interface

static pressure region), which would contribute to a reduction in the total pressure and flow angle along the contraction cone. In addition, non-uniformity in the leak circumferentially, would result in non-uniformity in the circumferential measurements.

Sealing of the gap, using strips of upholstery piping, resulted in the data given in Tables 1-17. Noted were:

1. An increase in flow angle  $\beta_2$  by approximately  $4^\circ$  (Figs. 11 and 12) and improvement in the total pressure distribution (Figs. 13 and 14).
2. Satisfactory circumferential uniformity in flow angle (Figs. 15 and 16) and total pressure (Figs. 17 and 18).

3. The effect of the jet wall spacing on  $\beta_2$  (Fig. 19) approached more closely the design expectation (Fig. 29), the difference which remained will be discussed in the following subsection.

In Fig. 20 is shown the effect of JW spacing on the total pressure distribution at the location where the measurements were taken.

Figures 21 through 24 show the effect of the JW throttle setting on the flow angle (Figs. 21 and 22) and on the total pressure (Figs. 23 and 24), for the two JW spacings at which reliable (leak-free) measurements were taken

Figures 25 through 28 show circumferential measurements of the flow angle and the total pressure distributions for the jet walls in the fully retracted position.

## B. THEORY AND EXPERIMENT

In Fig. 29 are shown the results for the measured flow angle (averaged as described in Appendix C) and the values obtained in Appendix A, using the design calculation method, for the wall spacing at the time of the tests of 2.62". The experimental values are seen to be lower by 4° at maximum and 8° at minimum jet wall spacing.

The design calculation was based on an idealized flow-field and was immediately questioned. A complete control volume analysis (Appendix D) was carried out in order to take into account the geometry of the generating cylinder and the contributions of wall friction.

Examples of results are plotted in Fig. 29. The control volume analysis appears to agree well with the measured values when the JW's are widely spaced, but to predict a stronger effect of reducing the spacing than is actually measured. The significant differences between the idealized design predictions and the control volume analysis however, imply that the geometry of the generating cylinder surface and effects of friction need to be included in analyzing the flow. It is noted that the control volume analysis includes one unknown blockage factor, and one which must be input from measurements. Further examination needs to be made of the uncertainties in the analysis, in order to explain the differences in the slopes of the lines in Fig. 29.

Finally in Fig. 29 are shown the calculated flow angles corresponding to the design value of the diffuser wall spacing (2.0"). Clearly an increase of the wall spacing results in an increase of the flow angle. Any desired range of flow angle can be obtained by changing the width (or span) of the test diffuser.

## V. CONCLUSIONS

From the work reported, the following conclusions were drawn:

1. The proposed method of flow control works satisfactorily.
2. Sealing the jet wall gap is essential, in order to obtain the desired flow angles and circumferential flow symmetry. A method to provide sealing, at specific values of jet wall spacing must be designed in order to achieve the desired working range of diffuser inlet flow angle.
3. A review of the control volume analysis is necessary in order to explain the measured flow angles.
4. While results obtained with MERIDL were not unrealistic, the development of a computer code which will accept the proper boundary conditions, for the CDTD, is needed in order to predict more accurately the distributions of flow conditions at the test section inlet.

An advanced code with transonic flow capability is required ultimately for the design of a high speed version of the CDTD.

TABLE 1  
FLOW CONDITIONS CALCULATED AT THE SURFACE OF THE  
GENERATING CYLINDER FOR MERIDL MODEL CHCK

$\beta_1$ SL	60°		65°		70°		75°	
	$V_1$	$\beta_1$	$V_1$	$\beta_1$	$V_1$	$\beta_1$	$V_1$	$\beta_2$
.00	220.17	83.41	229.86	84.71	237.92	85.92	244.26	87.06
.05	220.46	83.01	230.11	84.35	238.14	85.59	244.45	86.75
.1	220.69	82.59	230.28	83.99	238.14	85.27	244.57	86.48
.15	220.87	82.21	230.41	83.67	238.34	85.02	244.53	86.27
.20	221.08	88.81	230.54	83.34	238.37	84.78	244.24	86.09
.25	221.39	81.26	230.75	82.90	238.56	84.44	244.69	85.85
.30	221.78	80.64	231.02	82.40	238.72	84.06	244.80	85.59
.35	222.14	80.07	231.27	81.95	238.12	83.71	244.87	85.34
.40	222.44	79.60	231.53	81.57	239.18	83.41	244.94	85.11

UNITS

In Tables 1-17, velocity [V] is in ft/sec, angle [ $\beta$ ] is in degrees, displacement (L2) is in inches and the reading of the inclined manometer (DP) showing the difference between impact and atmospheric pressure--is in inches of water.

TABLE 2 (WEST)  
JW SPACING: 24.375 IN  
THROTTLES: "OPEN"

RUN	L2	DP	BETA	V	VR	VT	VTM
CDTI28	0.00	0.00	0.00	0.00	0.00	0.00	0.00
CDTI28	.15	7.05	58.20	115.15	60.68	97.86	80.86
CDTI28	.35	10.55	54.60	140.86	81.60	114.82	127.57
CDTI28	.75	12.15	55.60	151.16	85.40	124.73	145.04
CDTI28	1.25	11.85	56.80	149.29	81.74	124.92	139.04
CDTI28	1.75	11.80	57.40	148.97	80.26	125.50	137.16
CDTI28	2.15	11.05	58.20	144.16	75.97	122.52	126.73
CDTI28	2.35	8.65	60.40	127.55	63.00	110.90	95.14
CDTI28	2.62	0.00	0.00	0.00	0.00	0.00	0.00

AREA AVERAGED OVERALL VELOCITY 134.82  
AREA AVERAGED RADIAL VELOCITY 73.44  
MASS AVERAGED RADIAL VELOCITY 78.84  
MASS AVERAGED TANGENTIAL VELOCITY 120.77  
BLOCKAGE FACTOR .93  
AVERAGED FLOW ANGLE 56.86

TABLE 3 (BOTTOM)  
JW SPACING: 24.375 IN  
THROTTLES: "OPEN"

RUN	L2	DP	BETA	V	VR	VT	VTM
CDTI29	0.00	0.00	0.00	0.00	0.00	0.00	0.00
CDTI29	.15	6.65	60.80	111.83	54.56	97.62	72.91
CDTI29	.35	9.70	57.20	135.07	73.17	113.53	113.71
CDTI29	.75	11.55	56.00	147.38	82.42	122.19	137.85
CDTI29	1.25	11.30	56.20	145.78	81.10	121.14	134.48
CDTI29	1.75	11.50	56.00	147.06	82.24	121.92	137.26
CDTI29	2.15	10.55	55.00	140.86	80.79	115.39	127.62
CDTI29	2.35	8.55	56.00	126.81	70.91	105.13	102.05
CDTI29	2.62	0.00	0.00	0.00	0.00	0.00	0.00

AREA AVERAGED OVERALL VELOCITY 131.79  
AREA AVERAGED RADIAL VELOCITY 73.05  
MASS AVERAGED RADIAL VELOCITY 78.37  
MASS AVERAGED TANGENTIAL VELOCITY 117.24  
BLOCKAGE FACTOR .93  
AVERAGED FLOW ANGLE 56.24



TABLE 4 (EAST)  
JW SPACING: 24.375 IN  
THROTTLES: "OPEN"

RUN	L2	DP	BETA	V	VF	VT	VTM
CDTD30	0.00	0.00	0.00	0.00	0.00	0.00	0.00
CDTD30	.15	5.40	68.40	100.78	37.10	93.70	51.02
CDTD30	.35	9.10	60.60	130.82	64.22	113.97	107.44
CDTD30	.75	11.40	59.00	146.42	75.41	125.51	138.93
CDTD30	1.25	11.40	59.80	146.42	73.65	126.55	136.82
CDTD30	1.75	11.88	57.80	149.47	79.65	126.48	147.88
CDTD30	2.15	11.50	56.40	147.06	81.38	122.49	146.33
CDTD30	2.35	9.80	56.80	135.76	74.34	113.60	123.95
CDTD30	2.62	0.00	0.00	0.00	0.00	0.00	0.00

AREA AVERAGED OVERALL VELOCITY 132.53  
AREA AVERAGED RADIAL VELOCITY 68.13  
MASS AVERAGED RADIAL VELOCITY 74.00  
MASS AVERAGED TANGENTIAL VELOCITY 121.85  
BLOCKAGE FACTOR .92  
AVERAGED FLOW ANGLE 58.73

TABLE 5 (TOP)  
JW SPACING: 24.375 IN  
THROTTLES: "OPEN"

RUN	L2	DP	BETA	V	VF	VT	VTM
CDTD31	0.00	0.00	0.00	0.00	0.00	0.00	0.00
CDTD31	.15	6.70	62.40	112.25	52.01	99.48	78.00
CDTD31	.35	10.05	58.00	137.48	72.85	116.59	128.06
CDTD31	.75	11.60	57.40	147.70	79.58	124.43	149.29
CDTD31	1.25	11.10	58.00	144.48	76.56	122.53	141.44
CDTD31	1.75	11.00	58.60	143.83	74.94	122.77	138.71
CDTD31	2.15	9.20	60.00	131.54	65.77	113.92	112.96
CDTD31	2.35	6.85	64.60	113.50	48.69	102.53	75.26
CDTD31	2.62	0.00	0.00	0.00	0.00	0.00	0.00

AREA AVERAGED OVERALL VELOCITY 129.00  
AREA AVERAGED RADIAL VELOCITY 66.33  
MASS AVERAGED RADIAL VELOCITY 71.97  
MASS AVERAGED TANGENTIAL VELOCITY 118.66  
BLOCKAGE FACTOR .92  
AVERAGED FLOW ANGLE 58.76

TABLE 6 (WEST)  
JW SPACING: 24.375 IN  
THROTTLES: CLOSED

RUN	L2	DP	BETA	V	VR	VT	VTM
CDTD37	0.00	0.00	90.00	0.00	0.00	0.00	0.00
CDTD37	.15	6.70	66.40	112.25	44.94	102.86	67.20
CDTD37	.35	10.50	60.00	140.53	70.26	121.70	124.29
CDTD37	.75	12.80	58.00	155.15	82.22	131.58	157.25
CDTD37	1.25	12.55	59.00	153.63	79.13	131.69	151.46
CDTD37	1.75	12.60	59.20	153.94	78.82	132.23	151.50
CDTD37	2.15	11.30	60.40	145.78	72.01	126.76	132.67
CDTD37	2.35	9.20	64.00	131.54	57.66	118.23	99.09
CDTD37	2.62	0.00	90.00	0.00	0.00	0.00	0.00

AREA AVERAGED OVERALL VELOCITY 137.60  
AREA AVERAGED RADIAL VELOCITY 68.80  
MASS AVERAGED RADIAL VELOCITY 74.62  
MASS AVERAGED TANGENTIAL VELOCITY 127.68  
BLOCKAGE FACTOR .92  
AVERAGED FLOW ANGLE 59.70

TABLE 7 (TOP)  
JW SPACING: 24.375 IN  
THROTTLES: CLOSED

RUN	L2	DP	BETA	V	VR	VT	VTM
CDTI38	0.00	0.00	90.00	0.00	0.00	0.00	0.00
CDTI38	.15	7.15	66.00	115.96	47.17	105.94	69.48
CDTI38	.35	11.15	60.00	144.81	72.40	125.41	126.26
CDTI38	.75	13.60	58.70	159.93	83.09	136.65	157.88
CDTI38	1.25	13.10	59.00	156.96	80.84	134.54	151.24
CDTD38	1.75	13.30	59.00	158.16	81.46	135.57	153.55
CDTI38	2.15	12.65	59.40	154.24	78.52	132.76	144.95
CDTD38	2.35	10.70	61.20	141.86	68.34	124.31	118.13
CDTI38	2.62	0.00	90.00	0.00	0.00	0.00	0.00

AREA AVERAGED OVERALL VELOCITY 142.54  
AREA AVERAGED RADIAL VELOCITY 71.92  
MASS AVERAGED RADIAL VELOCITY 77.56  
MASS AVERAGED TANGENTIAL VELOCITY 131.72  
BLOCKAGE FACTOR .93  
AVERAGED FLOW ANGLE 59.51

TABLE 8 (BOTTOM)  
JW SPACING: 24.375 IN  
THROTTLES: CLOSED

RUN	L2	DP	BETA	V	VF	VT	VTM
CDTI39	0.00	0.00	90.00	0.00	0.00	0.00	0.00
CDTI39	.15	8.70	62.00	127.91	60.05	112.94	87.24
CDTI39	.35	12.50	57.40	153.33	82.61	129.17	137.24
CDTI39	.75	13.95	57.40	161.97	87.27	136.46	153.16
CDTI39	1.25	13.35	57.60	158.45	84.90	133.79	146.10
CDTI39	1.75	13.55	57.80	159.64	85.07	135.08	147.80
CDTI39	2.15	12.90	56.20	155.76	86.65	129.43	144.25
CDTI39	2.35	10.50	57.40	140.53	75.71	118.39	115.28
CDTI39	2.62	0.00	90.00	0.00	0.00	0.00	0.00

AREA AVERAGED OVERALL VELOCITY 145.27  
AREA AVERAGED RADIAL VELOCITY 77.75  
MASS AVERAGED RADIAL VELOCITY 83.23  
MASS AVERAGED TANGENTIAL VELOCITY 130.94  
BLOCKAGE FACTOR .93  
AVERAGED FLOW ANGLE 57.56

TABLE 9 (EAST)  
JW SPACING: 24.375 IN  
THROTTLES: CLOSED

RUN	L2	DP	BETA	V	VF	VT	VTM
CDTI40	0.00	0.00	90.00	0.00	0.00	0.00	0.00
CDTI40	.15	8.45	66.20	126.06	50.87	115.34	83.05
CDTI40	.35	11.80	61.00	148.97	72.22	130.29	133.18
CDTI40	.75	14.30	59.40	163.99	83.43	141.16	166.78
CDTI40	1.25	14.30	59.40	163.99	83.43	141.16	166.78
CDTI40	1.75	14.45	60.00	164.85	82.43	142.77	166.55
CDTI40	2.15	12.40	61.80	152.71	72.16	134.58	137.48
CDTI40	2.35	9.10	66.20	130.82	52.79	119.70	89.44
CDTI40	2.62	0.00	90.00	0.00	0.00	0.00	0.00

AREA AVERAGED OVERALL VELOCITY 145.70  
AREA AVERAGED RADIAL VELOCITY 70.65  
MASS AVERAGED RADIAL VELOCITY 76.96  
MASS AVERAGED TANGENTIAL VELOCITY 126.86  
BLOCKAGE FACTOR .92  
AVERAGED FLOW ANGLE 60.64

TABLE 10 (WEST)  
JW SPACING: 8.0 IN  
THROTTLES: CLOSED

RUN	L2	DP	BETA	V	VP	VT	VTM
CDTD81	0.00	0.00	90.00	0.00	0.00	0.00	0.00
CDTD81	.15	4.20	82.00	88.88	12.37	88.01	36.86
CDTD81	.35	4.90	80.80	96.00	15.35	94.76	49.25
CDTD81	.75	6.55	74.60	110.99	29.47	107.00	106.80
CDTD81	1.25	8.65	67.60	127.55	48.60	117.92	194.08
CDTD81	1.75	8.10	69.20	123.42	43.83	115.38	171.24
CDTD81	2.15	5.15	75.40	98.42	24.81	95.24	80.00
CDTD81	2.35	3.75	78.00	83.98	17.46	82.14	48.57
CDTD81	2.62	0.00	90.00	0.00	0.00	0.00	0.00

AREA AVERAGED OVERALL VELOCITY 102.59  
 AREA AVERAGED RADIAL VELOCITY 29.53  
 MASS AVERAGED RADIAL VELOCITY 36.93  
 MASS AVERAGED TANGENTIAL VELOCITY 108.91  
 BLOCKAGE FACTOR .80  
 AVERAGED FLOW ANGLE 71.27

TABLE 11 (TOP)  
JW SPACING: 8.0 IN  
THROTTLES: CLOSED

RUN	L2	DP	BETA	V	VP	VT	VTM
CDTD82	0.00	0.00	90.00	0.00	0.00	0.00	0.00
CDTD82	.15	3.00	79.00	75.11	14.33	73.73	39.54
CDTD82	.35	3.95	77.00	86.19	19.39	83.98	60.92
CDTD82	.75	6.45	71.00	110.14	35.86	104.14	139.71
CDTD82	1.25	8.05	67.60	123.04	46.89	113.76	199.57
CDTD82	1.75	6.45	73.20	110.14	31.83	105.44	125.58
CDTD82	2.15	5.00	81.60	96.97	14.17	95.93	50.84
CDTD82	2.35	4.05	84.60	87.27	8.21	86.89	26.70
CDTD82	2.62	0.00	90.00	0.00	0.00	0.00	0.00

AREA AVERAGED OVERALL VELOCITY 97.34  
 AREA AVERAGED RADIAL VELOCITY 26.73  
 MASS AVERAGED RADIAL VELOCITY 34.54  
 MASS AVERAGED TANGENTIAL VELOCITY 103.92  
 BLOCKAGE FACTOR .77  
 AVERAGED FLOW ANGLE 71.62

TABLE 12 (BOTTOM)

JW SPACING: 8.0 IN  
THROTTLES: CLOSED

RUN	L2	DP	BETA	V	VR	VT	VTM
CDTI83	0.00	0.00	90.00	0.00	0.00	0.00	0.00
CDTI83	.15	4.00	80.80	86.73	13.87	85.62	40.71
CDTD83	.35	4.80	79.40	95.01	19.10	93.07	60.97
CDTI83	.75	6.55	73.60	110.99	31.34	106.47	114.41
CDTD83	1.25	8.25	68.20	124.56	46.26	115.65	183.45
CDTD83	1.75	7.50	71.40	118.77	37.88	112.56	146.22
CDTD83	2.15	5.80	76.00	104.44	25.27	101.34	87.80
CDTI83	2.35	4.75	78.00	94.52	19.65	92.45	62.30
CDTD83	2.62	0.00	90.00	0.00	0.00	0.00	0.00

AREA AVERAGED OVERALL VELOCITY 102.64  
 AREA AVERAGED RADIAL VELOCITY 29.16  
 MASS AVERAGED RADIAL VELOCITY 34.63  
 MASS AVERAGED TANGENTIAL VELOCITY 107.62  
 BLOCKAGE FACTOR .84  
 AVERAGED FLOW ANGLE 72.16

TABLE 13 (EAST)

JW SPACING: 8.0 IN  
THROTTLES: CLOSED

RUN	L2	DP	BETA	V	VR	VT	VTM
CDTI84	0.00	0.00	90.00	0.00	0.00	0.00	0.00
CDTI84	.15	4.10	82.00	87.81	12.22	86.96	38.03
CDTD84	.35	5.05	80.00	97.46	16.92	95.97	58.13
CDTI84	.75	7.10	73.60	115.55	32.63	110.85	129.44
CDTI84	1.25	8.65	68.40	127.55	46.95	118.59	199.20
CDTI84	1.75	6.95	70.60	114.33	37.98	107.84	146.56
CDTD84	2.15	4.35	77.20	90.45	20.04	88.20	63.25
CDTD84	2.35	3.50	80.80	81.13	12.97	80.09	37.18
CDTI84	2.62	0.00	90.00	0.00	0.00	0.00	0.00

AREA AVERAGED OVERALL VELOCITY 100.74  
 AREA AVERAGED RADIAL VELOCITY 27.94  
 MASS AVERAGED RADIAL VELOCITY 35.03  
 MASS AVERAGED TANGENTIAL VELOCITY 107.74  
 BLOCKAGE FACTOR .80  
 AVERAGED FLOW ANGLE 71.99

TABLE 14 (EAST)  
JW SPACING: 8.0 IN  
THROTTLES: OPEN

RUN	L2	DP	BETA	V	VP	VT	VTM
CDTD86	0.00	0.00	0.00	0.00	0.00	0.00	0.00
CDTD86	.15	4.40	81.80	90.97	12.97	90.04	32.01
CDTD86	.35	5.95	77.20	105.78	23.44	103.15	66.24
CDTD86	.75	9.80	70.00	135.76	46.43	127.57	162.30
CDTD86	1.25	11.40	67.40	146.42	56.27	135.18	208.42
CDTI86	1.75	10.00	69.00	137.14	49.15	128.03	172.40
CDTD86	2.15	5.85	74.50	104.89	28.03	101.08	77.63
CDTD86	2.35	5.20	78.80	98.89	19.21	97.01	51.06
CDTD86	2.62	0.00	0.00	0.00	0.00	0.00	0.00

AREA AVERAGED OVERALL VELOCITY 116.57  
 AREA AVERAGED RADIAL VELOCITY 36.50  
 MASS AVERAGED RADIAL VELOCITY 44.56  
 MASS AVERAGED TANGENTIAL VELOCITY 123.43  
 BLOCKAGE FACTOR .82  
 AVERAGED FLOW ANGLE 70.15

TABLE 15 (BOTTOM)  
JW SPACING: 8.0 IN  
THROTTLES: OPEN

RUN	L2	DP	BETA	V	VP	VT	VTM
CDTD87	0.00	0.00	0.00	0.00	0.00	0.00	0.00
CDTD87	.15	5.65	81.60	103.08	15.06	101.98	40.60
CDTD87	.35	7.05	78.00	115.15	23.94	112.63	71.29
CDTI87	.75	9.55	70.00	134.02	45.84	125.94	152.62
CDTD87	1.25	11.05	67.40	144.16	55.40	133.09	194.95
CDTD87	1.75	9.75	68.00	135.41	50.73	125.55	168.40
CDTD87	2.15	6.15	72.40	107.55	32.52	102.51	88.14
CDTD87	2.35	4.60	74.00	93.01	25.64	89.41	60.61
CDTI87	2.62	0.00	0.00	0.00	0.00	0.00	0.00

AREA AVERAGED OVERALL VELOCITY 117.12  
 AREA AVERAGED RADIAL VELOCITY 37.82  
 MASS AVERAGED RADIAL VELOCITY 44.69  
 MASS AVERAGED TANGENTIAL VELOCITY 121.62  
 BLOCKAGE FACTOR .85  
 AVERAGED FLOW ANGLE 69.82

TABLE 16 (WEST)  
JW SPACING: 8.0 IN  
THROTTLES: OPEN

RUN	L2	DP	BETA	V	VR	VT	VTM
CDTD88	0.00	0.00	0.00	0.00	0.00	0.00	0.00
CDTD88	.15	3.30	82.20	78.78	10.69	78.05	22.20
CDTD88	.35	4.95	78.00	96.49	20.06	94.38	50.36
CDTD88	.75	9.60	69.60	134.37	46.84	125.94	156.90
CDTD88	1.25	11.85	67.10	149.29	58.09	137.52	212.49
CDTD88	1.75	11.05	68.60	144.16	52.60	134.22	187.79
CDTD88	2.15	7.90	74.60	121.89	32.37	117.51	101.18
CDTD88	2.35	5.95	78.80	105.78	20.55	103.77	56.71
CDTD88	2.62	0.00	0.00	0.00	0.00	0.00	0.00

AREA AVERAGED OVERALL VELOCITY 118.79  
AREA AVERAGED RADIAL VELOCITY 37.60  
MASS AVERAGED RADIAL VELOCITY 46.51  
MASS AVERAGED TANGENTIAL VELOCITY 126.62  
BLOCKAGE FACTOR .81  
AVERAGED FLOW ANGLE 69.83

TABLE 17 (TOP)  
JW SPACING: 8.0 IN  
THROTTLES: OPEN

RUN	L2	DP	BETA	V	VR	VT	VTM
CDTD89	0.00	0.00	0.00	0.00	0.00	0.00	0.00
CDTD89	.15	5.50	80.00	101.70	17.66	100.16	47.09
CDTD89	.35	7.10	76.00	115.55	27.96	112.12	83.44
CDTD89	.75	9.85	69.40	136.11	47.89	127.40	162.42
CDTD89	1.25	11.10	66.80	144.48	56.92	132.80	201.23
CDTD89	1.75	8.95	68.40	129.74	47.76	120.63	153.37
CDTD89	2.15	5.40	73.20	100.78	29.13	96.47	74.81
CDTD89	2.35	3.75	77.00	83.98	18.89	81.83	41.15
CDTD89	2.62	0.00	0.00	0.00	0.00	0.00	0.00

AREA AVERAGED OVERALL VELOCITY 114.87  
AREA AVERAGED RADIAL VELOCITY 37.56  
MASS AVERAGED RADIAL VELOCITY 44.82  
MASS AVERAGED TANGENTIAL VELOCITY 120.41  
BLOCKAGE FACTOR .84  
AVERAGED FLOW ANGLE 69.58



Figure 1. View of the CDTD



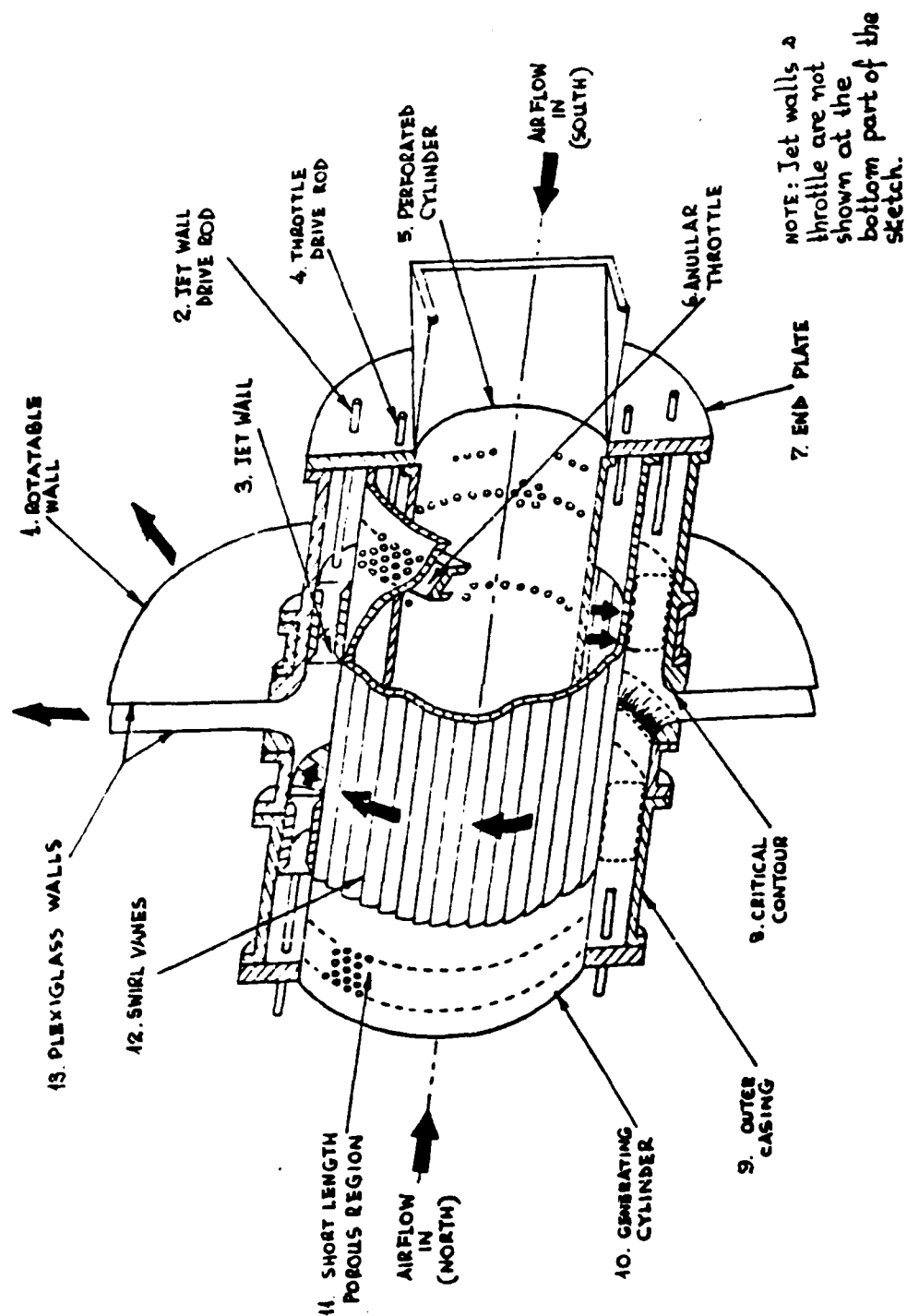


Figure 2. Schematic of CDTD Components

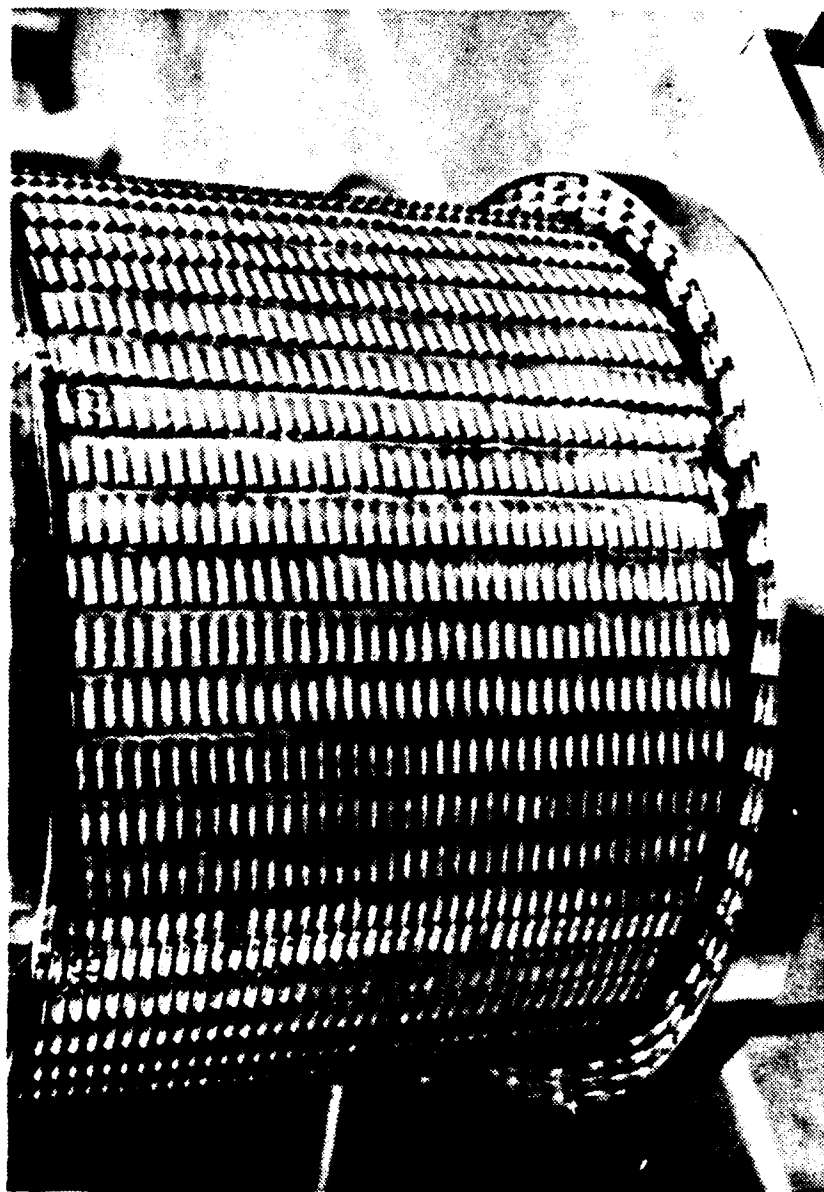


Figure 3. View of the Generating Cylinder and Jet Wall Hardware

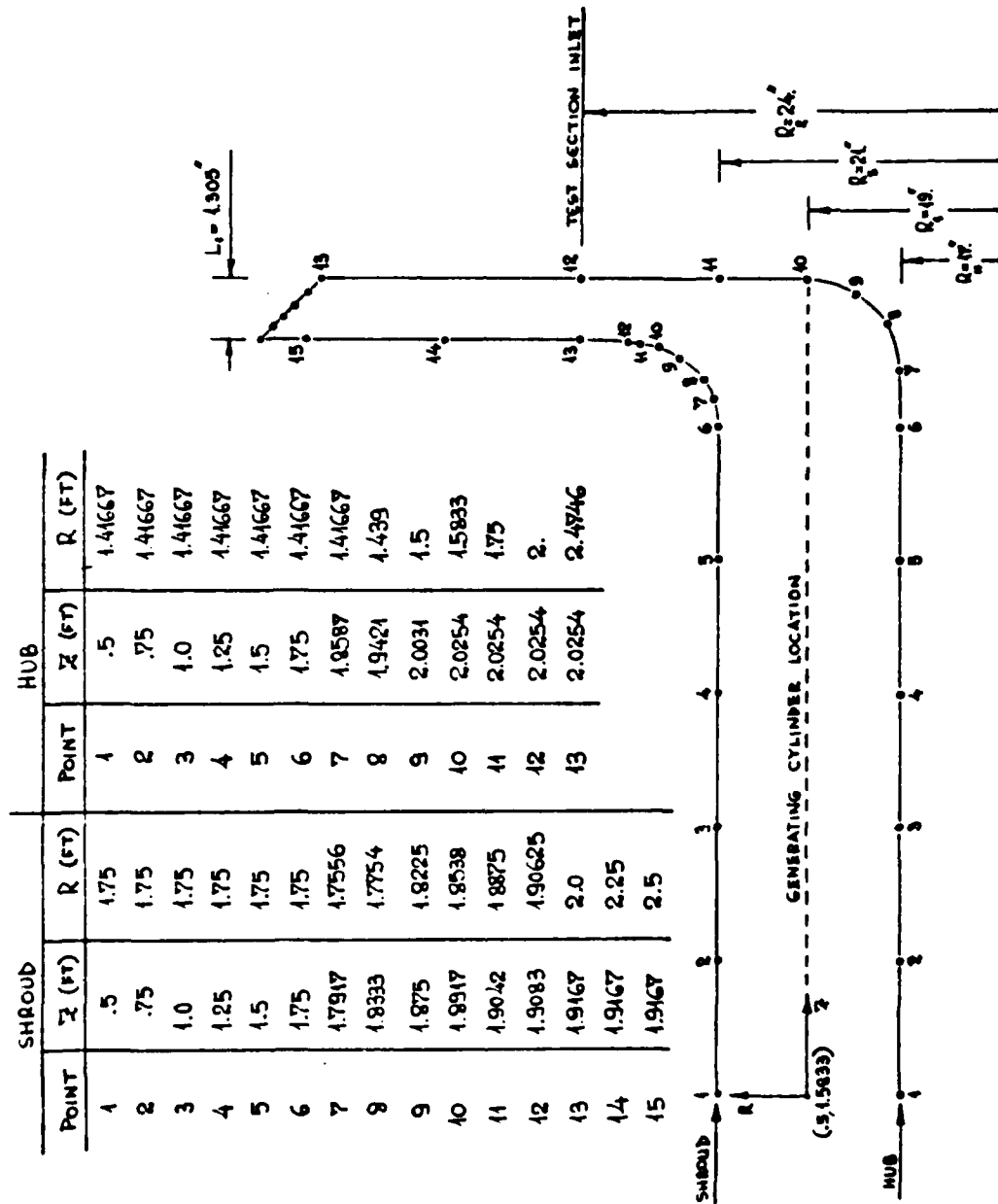


Figure 4. CDTD Flowfield Model for MERIDL

FIGURE 5a

STREAMLINES GENERATED BY MERIDIAN

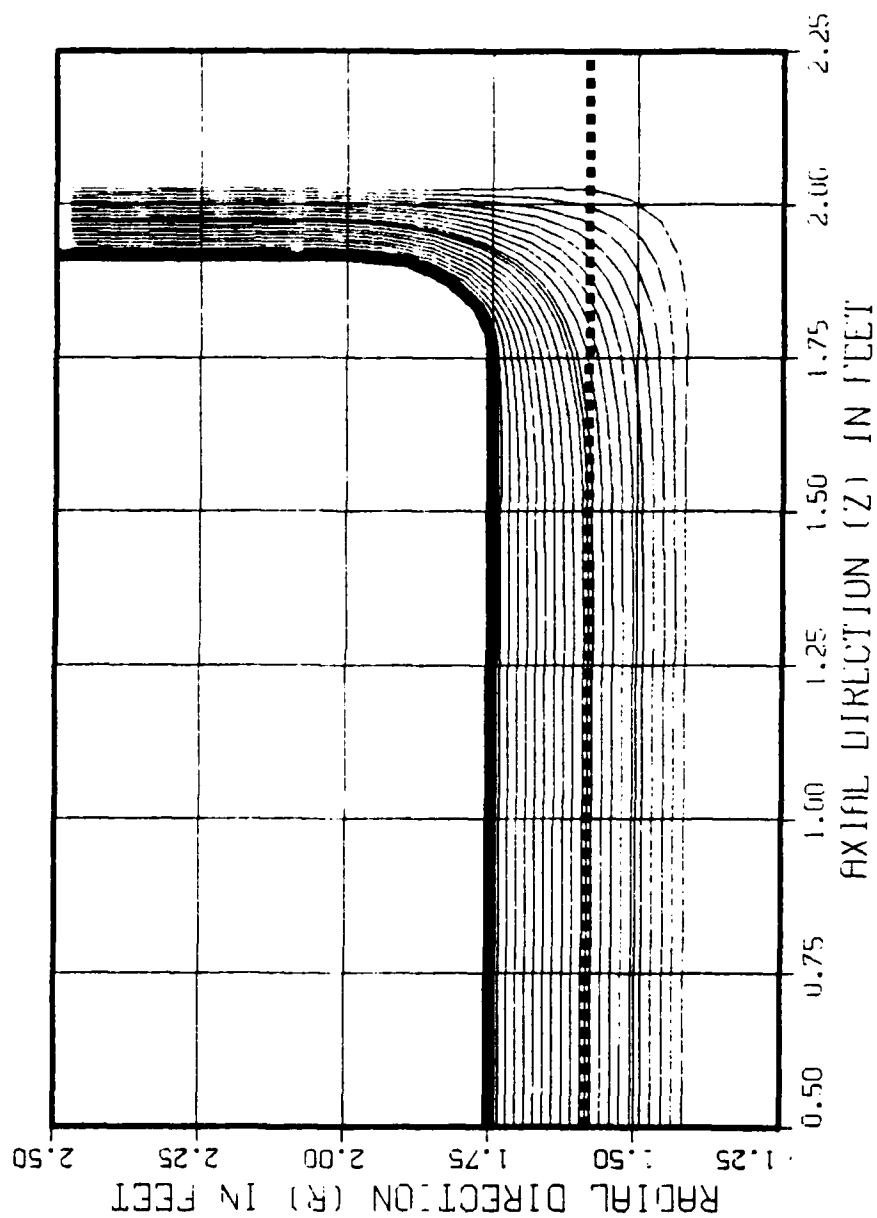


FIGURE 5b  
STREHLINES IN CONTRACTION CONE

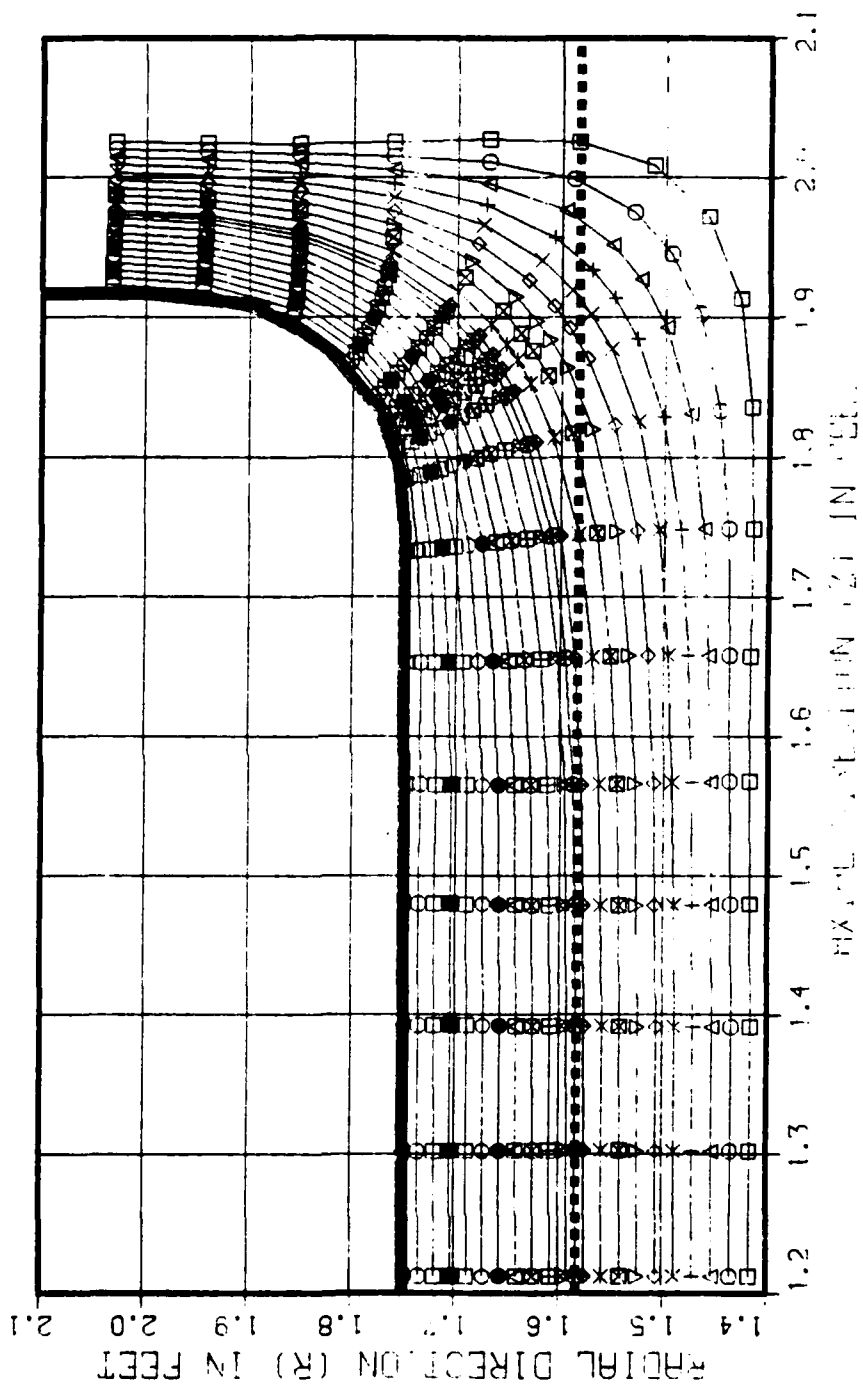


FIGURE 6  
TOTAL VELOCITY VARIATION  
ALONG CONTRACTION COURSE (STATIONS 14-24)

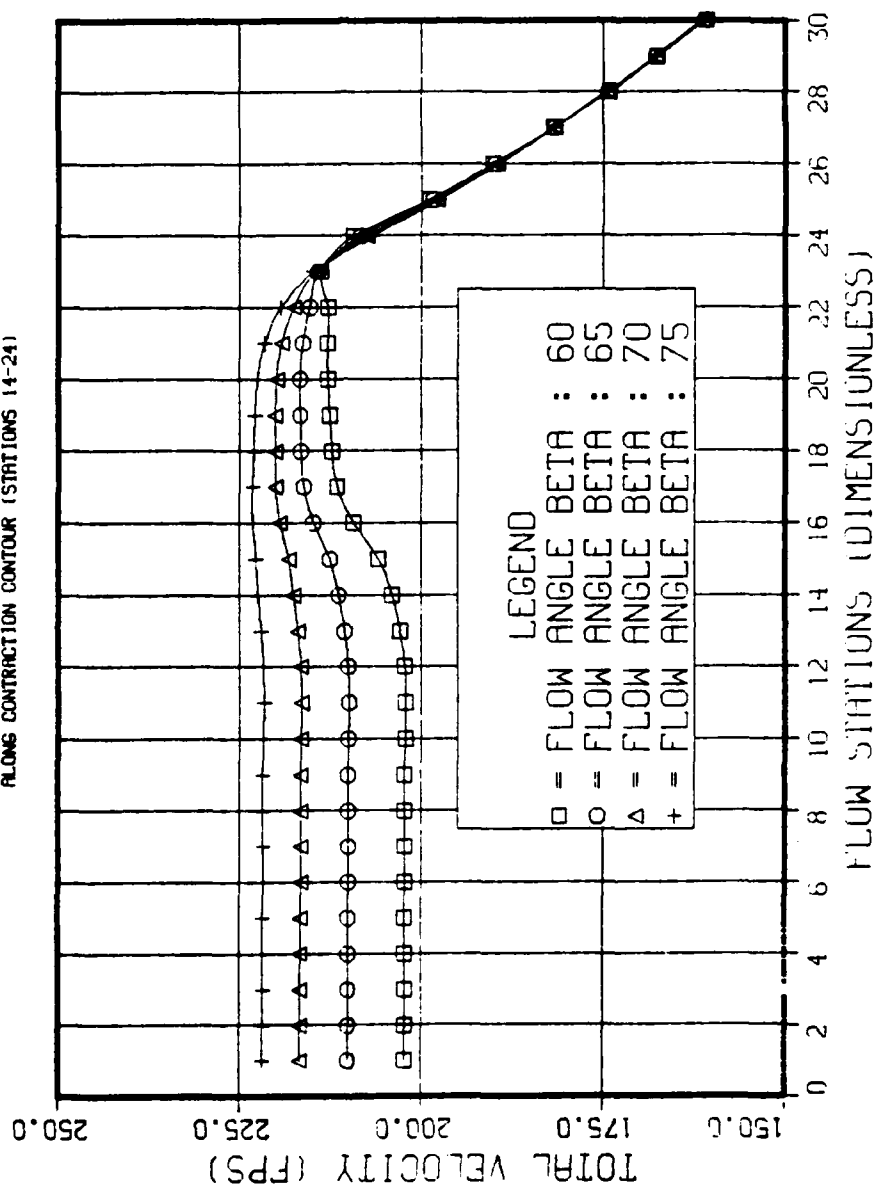


FIGURE 7  
TOTAL VELOCITY VARIATION  
ALONG - 0.0 (STATIONS 19-25)

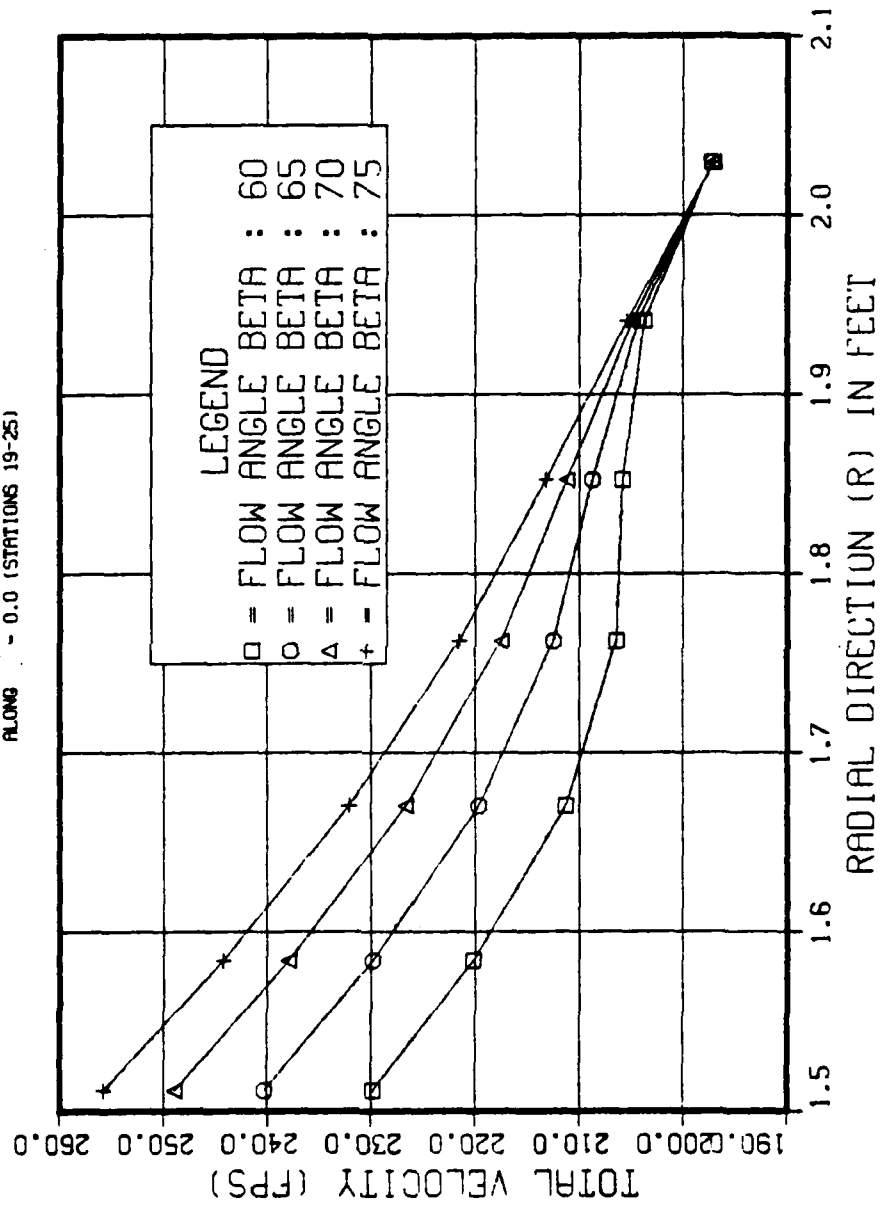
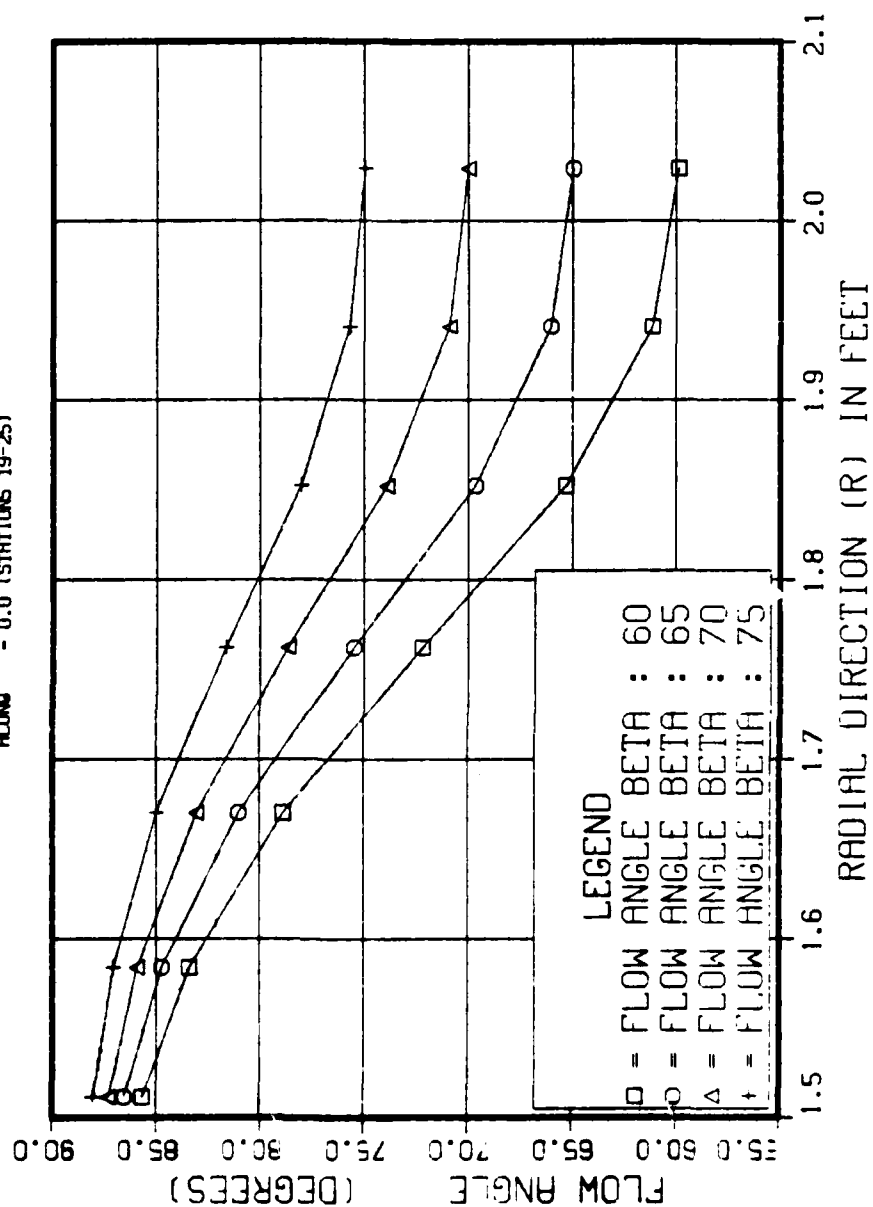


FIGURE 8  
FLOW ANGLE VARIATION  
ALONG - 0.0 (STATIONS 19-25)





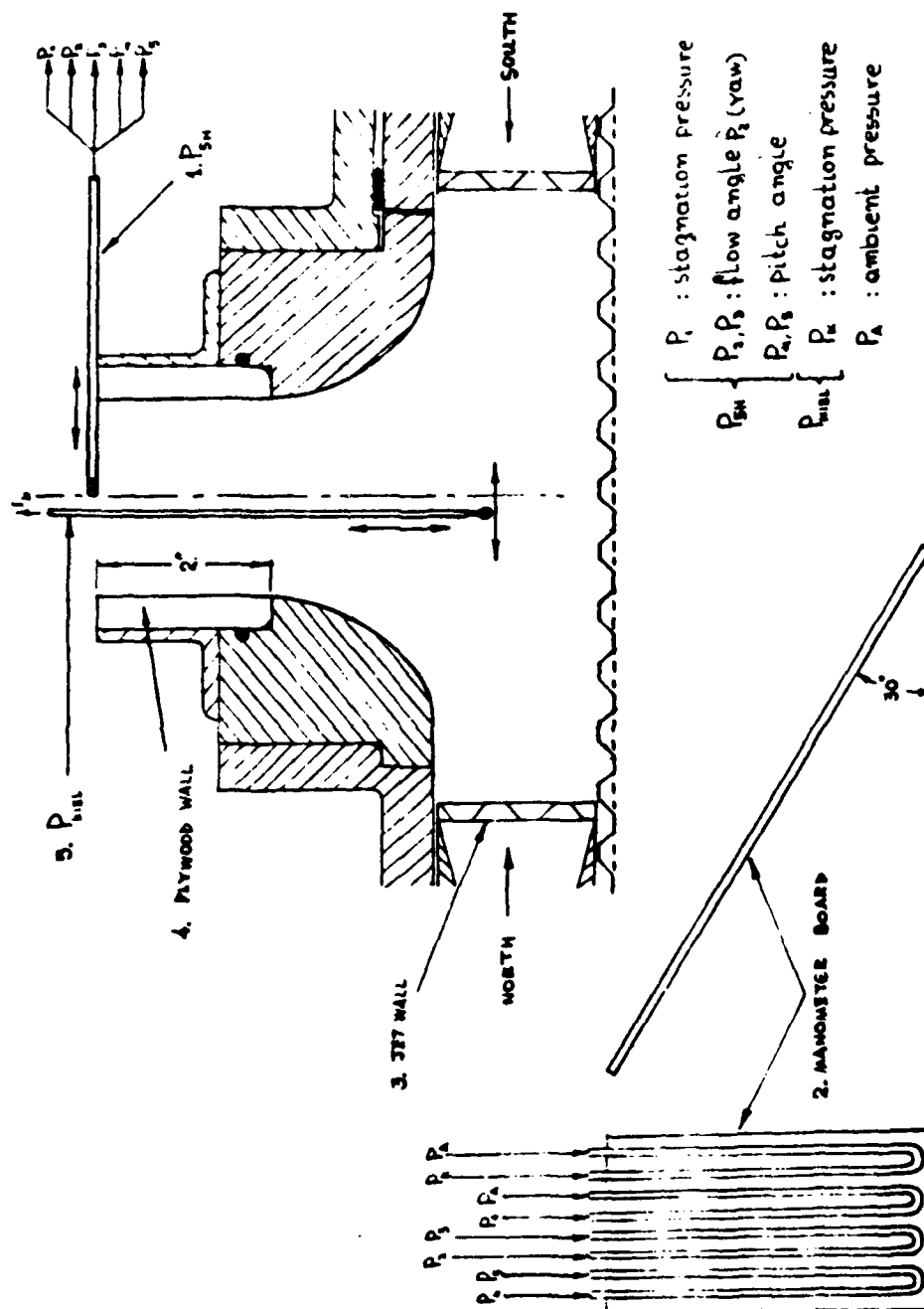


Figure 9. Installed Instrumentation for Preliminary Measurements

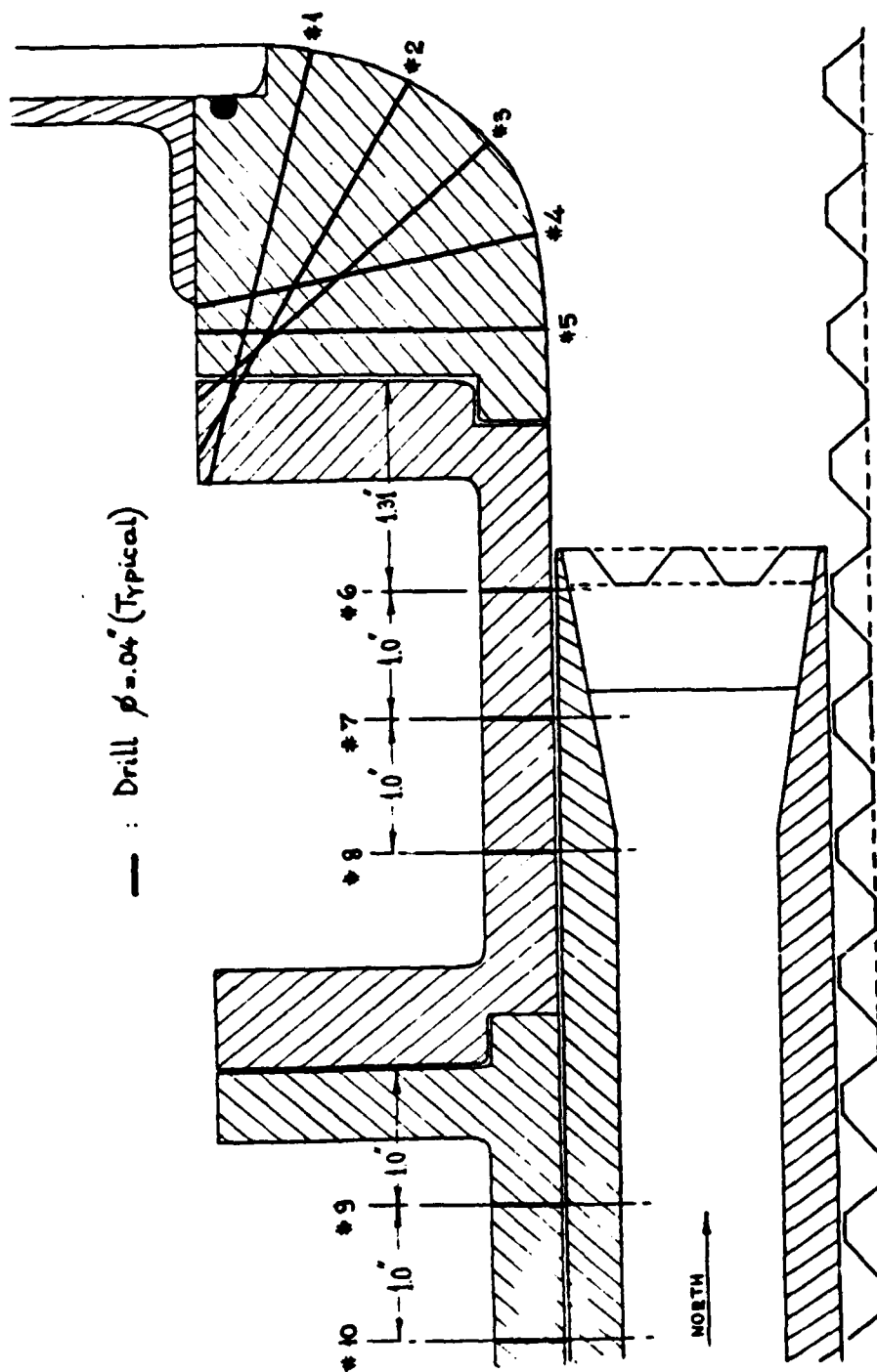


Figure 10a. Instrumentation Not Installed for Preliminary Measurements

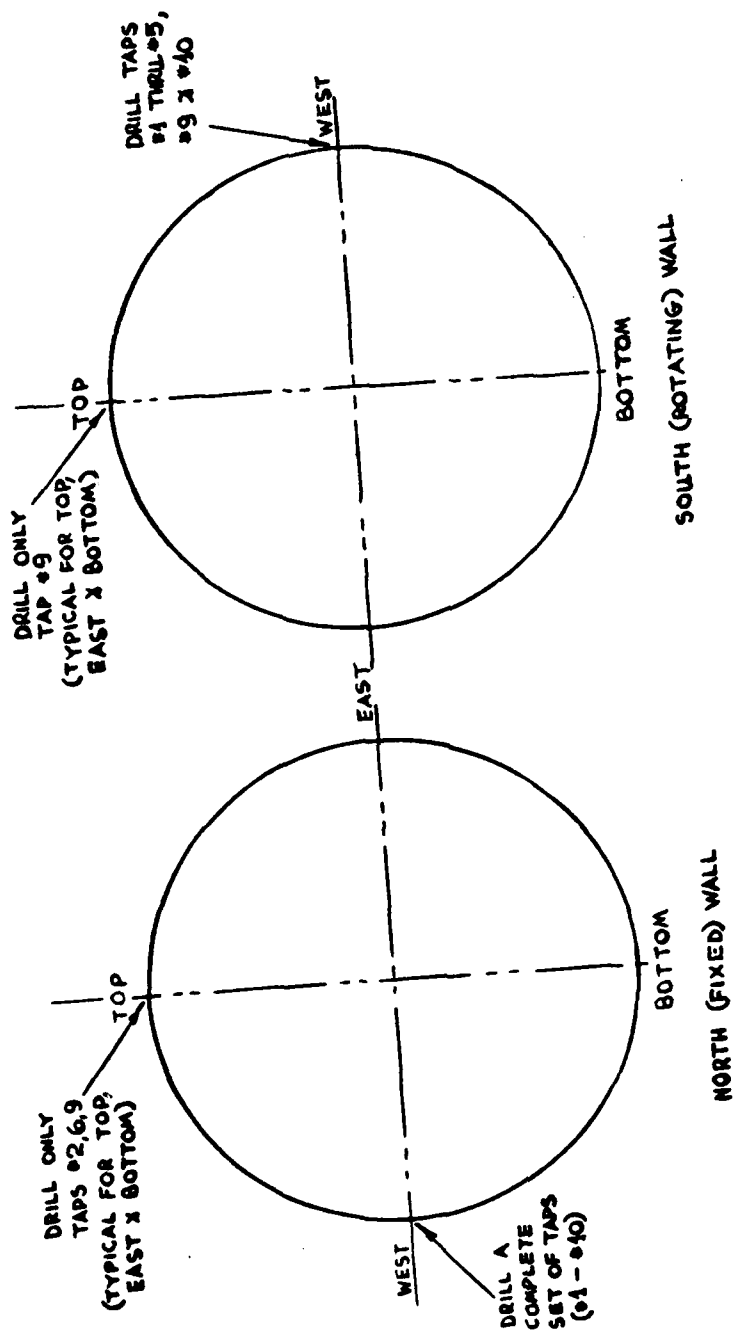


Figure 10b. Circumferential Arrangement of Pressure Taps

FIGURE 11

JW SEALING EFFECT IN FLOW ANGLE (WEST)

JW SPACING : 8.0, THROTTLES : OPEN

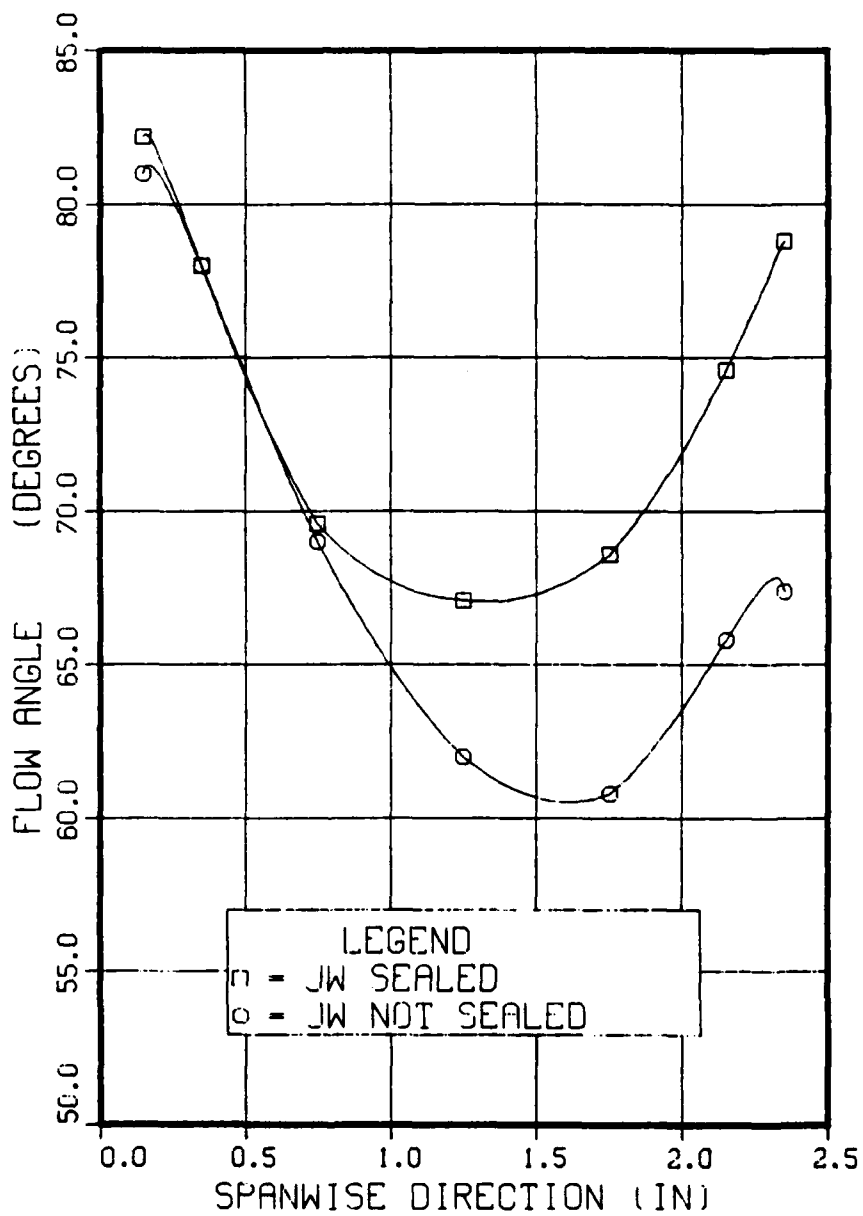


FIGURE 12

JW SEALING EFFECT IN FLOW ANGLE (WEST)

JW SPACING : 8.0, THROTTLES : CLOSED

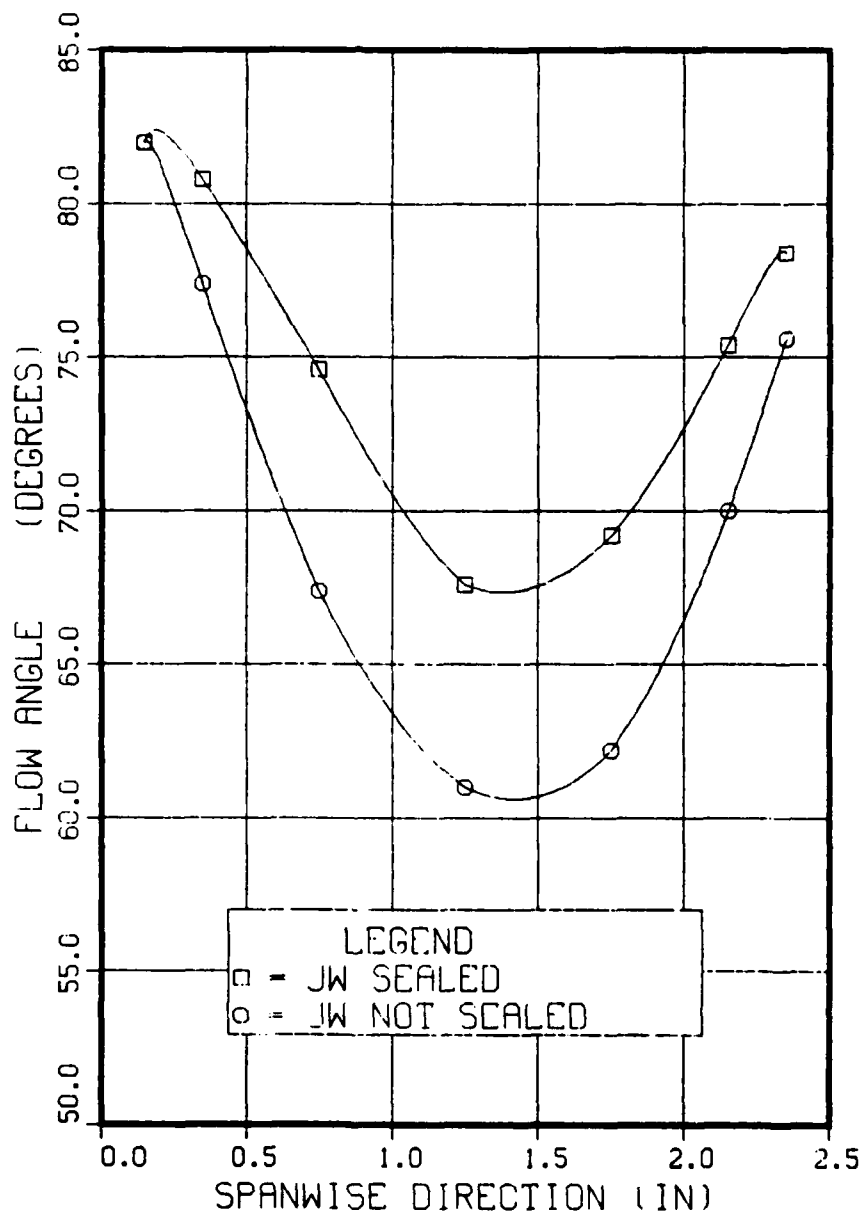


FIGURE 13

JW SEALING EFFECT IN TOTAL PRESSURE (WEST)

JW SPACING : 8.0, THROTTLES : OPEN

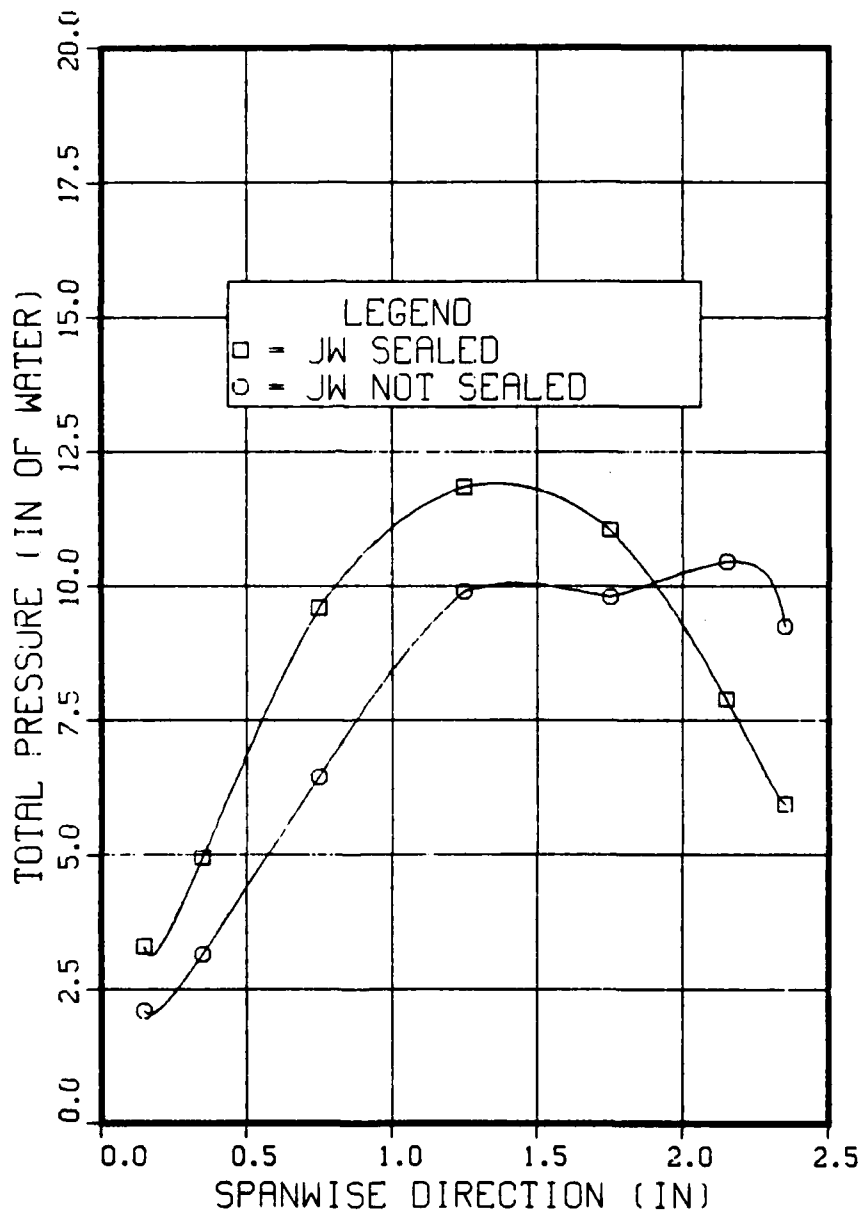
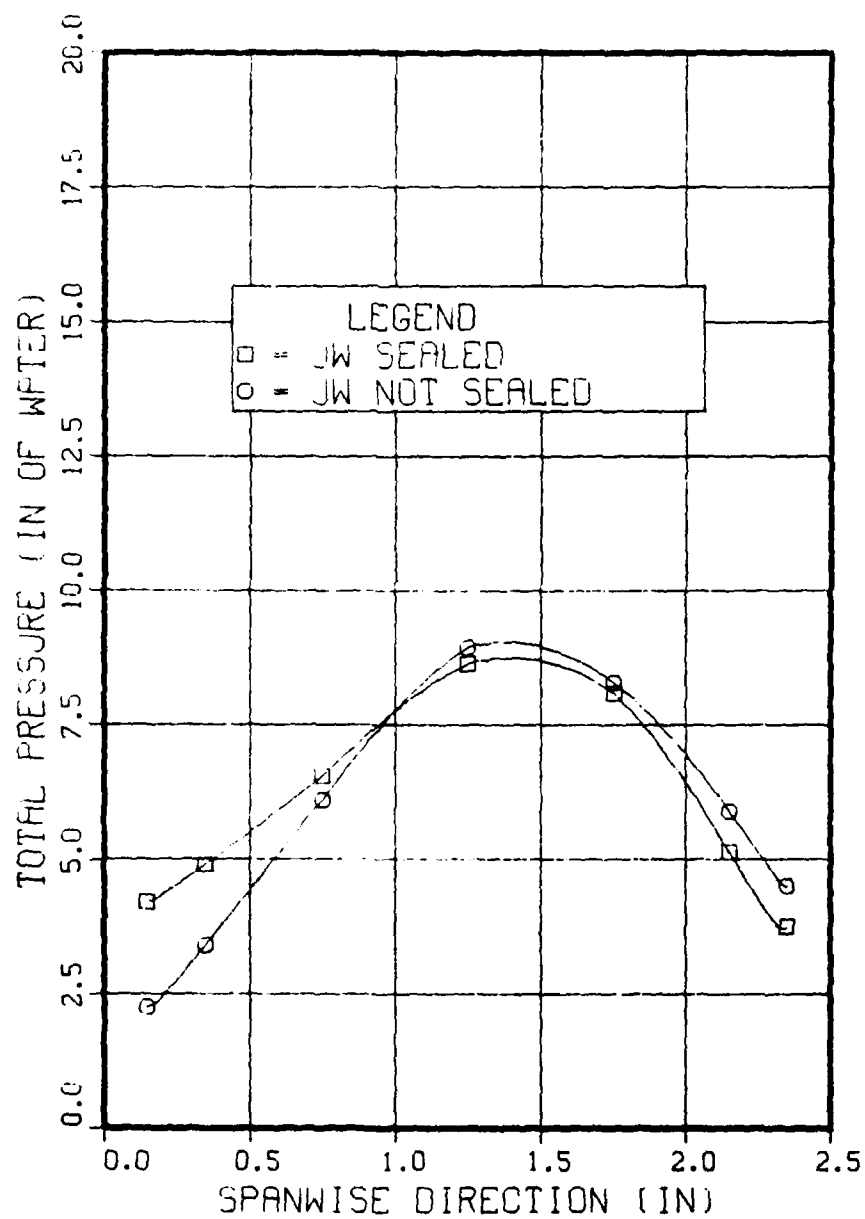


FIGURE 14

JW SEALING EFFECT IN TOTAL PRESSURE (WEST)

JW LEAKING : 5.0, THROTTLES : CLOSED



# FIGURE 15

CUMULATIVE MEASUREMENTS - FLOW ANGLE

W. SPACING : 1.0 IN. THROTTLES : OPEN

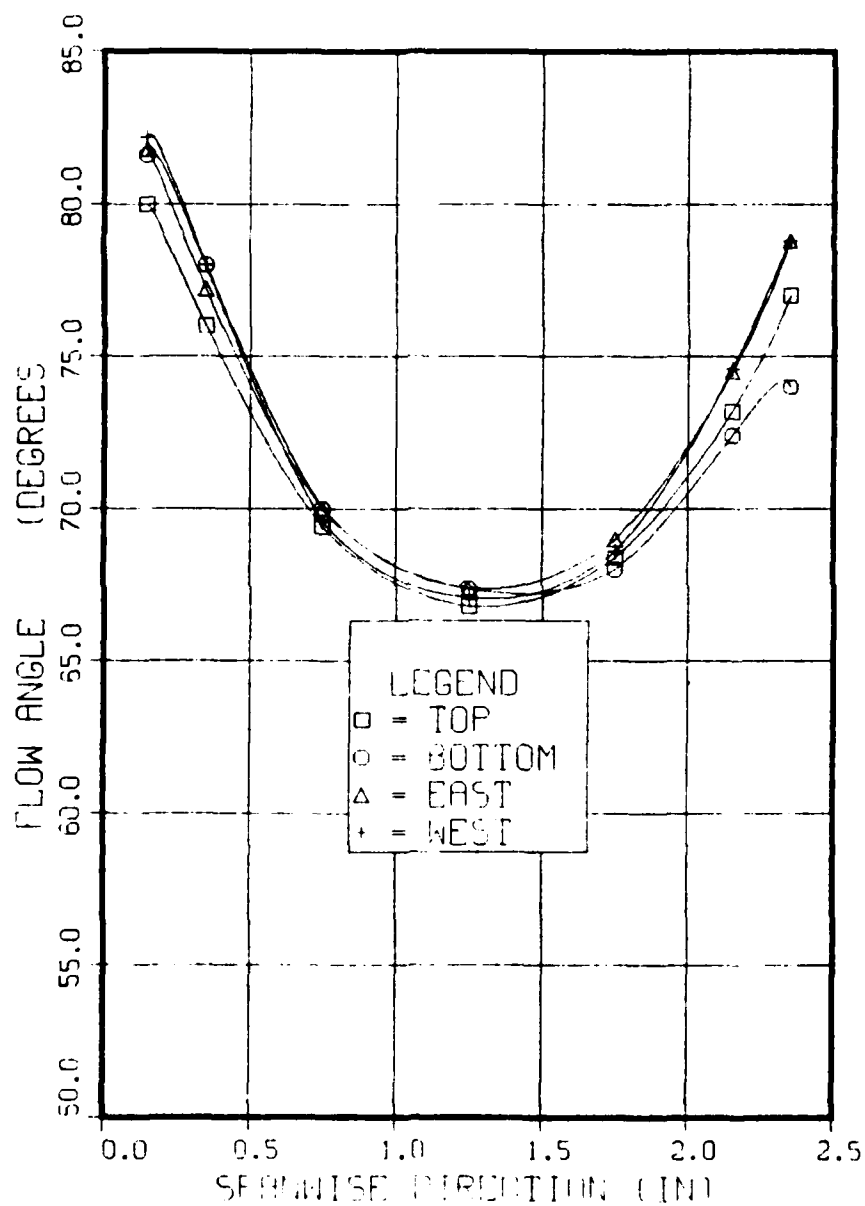




# Figure 16

COMPARISON OF EXPERIMENTAL AND CALCULATED  
WINGING ANGLES, PROFILES CLOSED

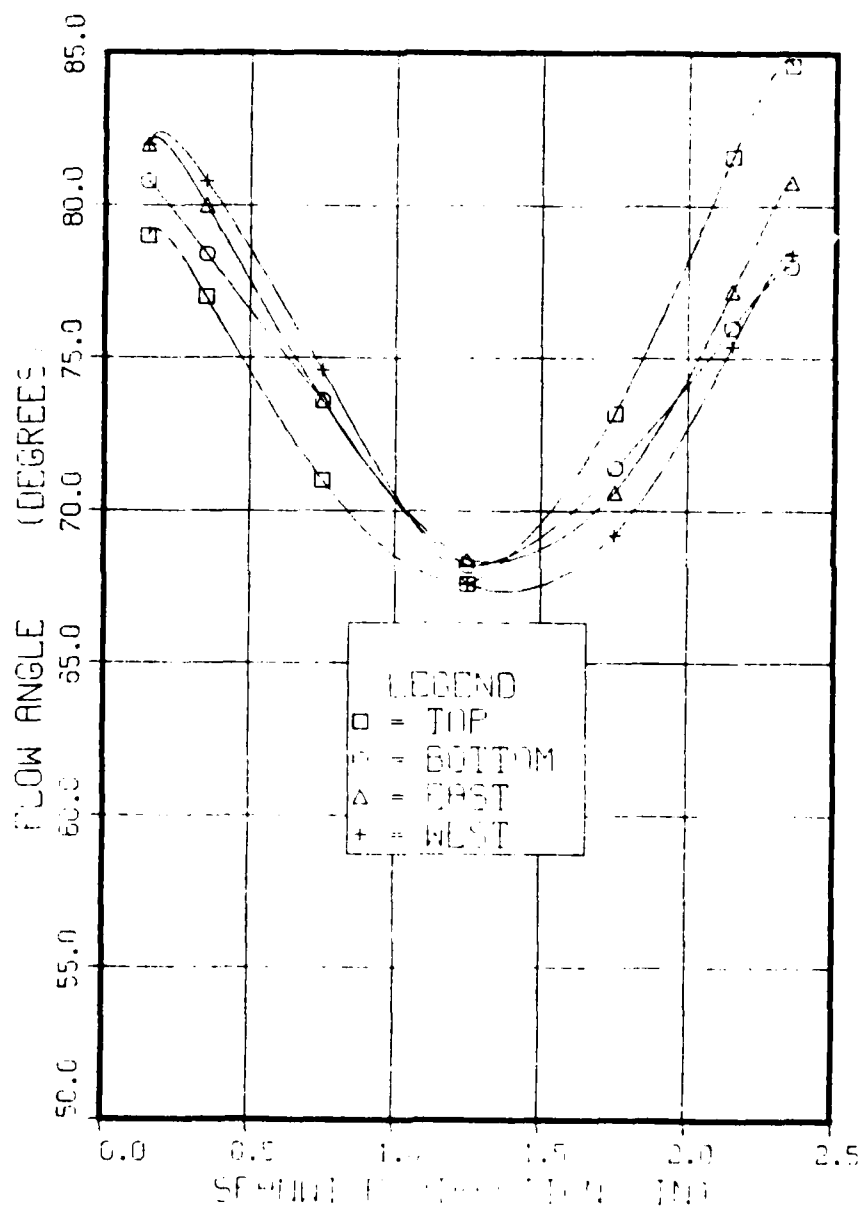
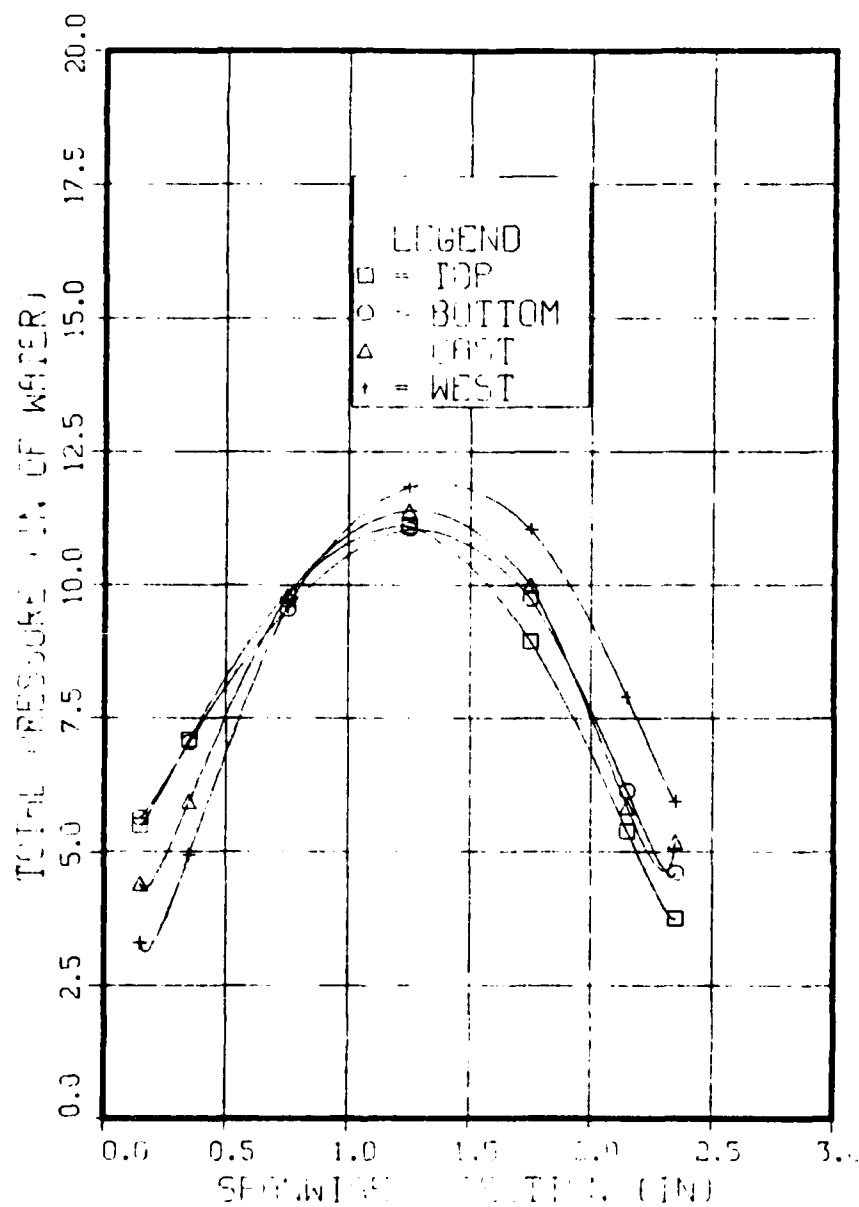


# FIGURE 17

DIFFERENTIAL MEASUREMENT PRESSURE

SPACING 1.0 IN. THROTTLES OPEN



CIRCUMFERENTIAL MEASUREMENTS (PRESSURE)

WINDING : 8.0 IN THROTTLE : CLOSED

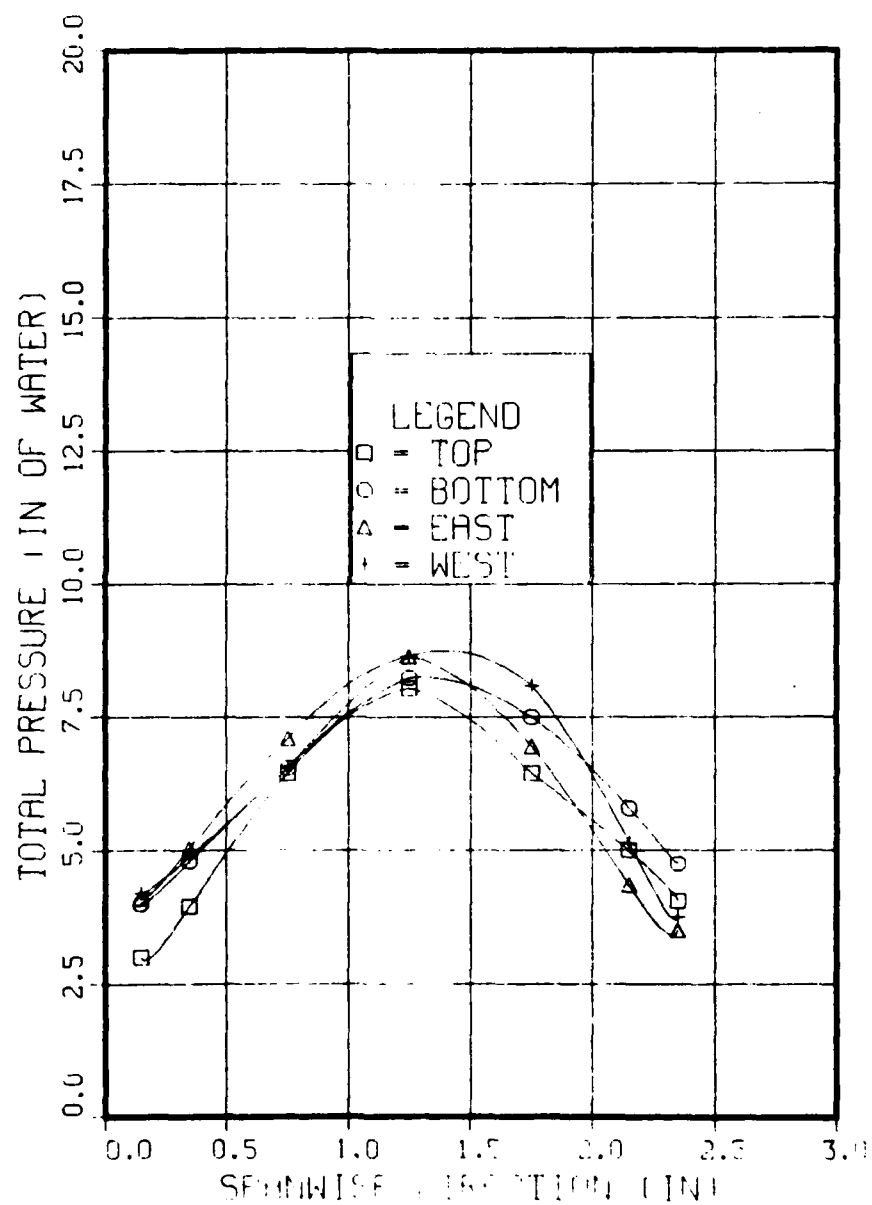
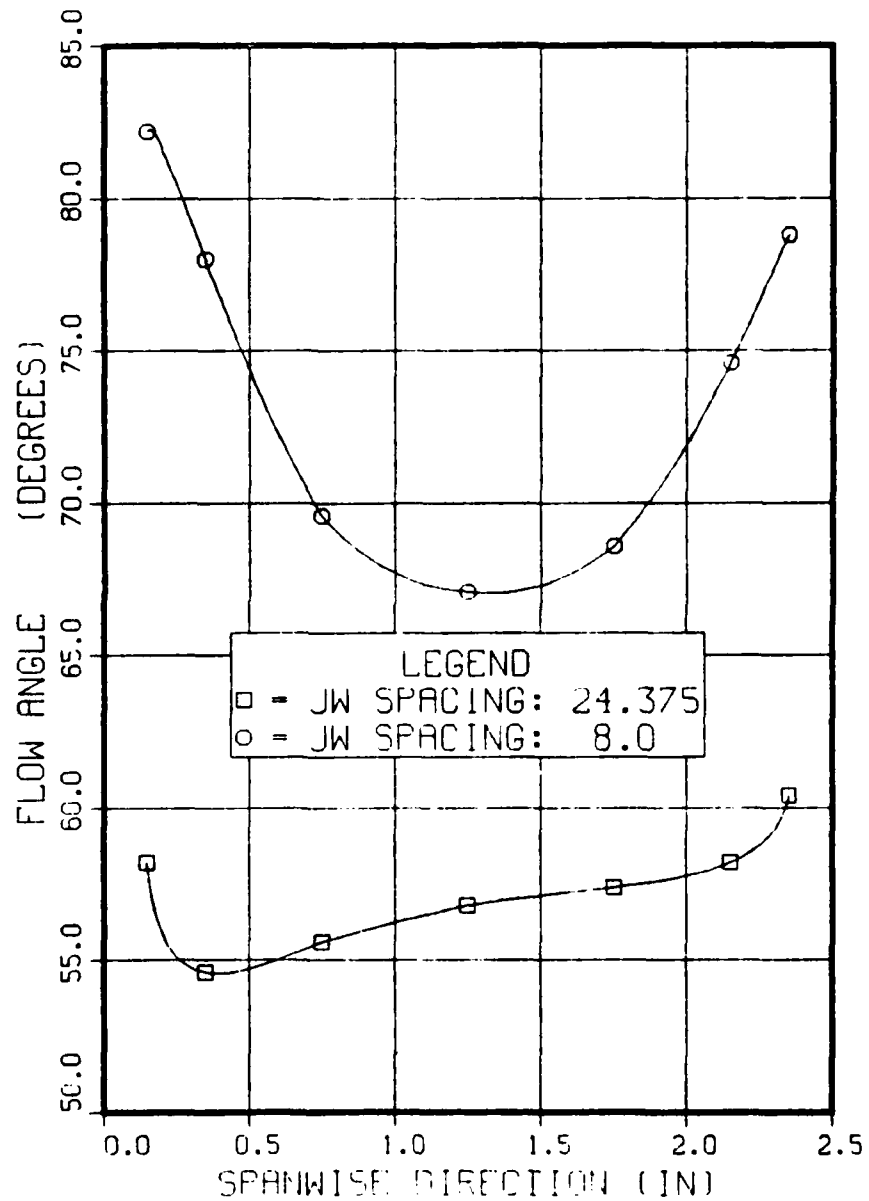


FIGURE 19

JW SPACING EFFECT IN FLOW ANGLE (WEST)

THROTTLES : OPEN



# FIGURE 20

ON SPACING EFFECT ON TOTAL PRESSURE (WEST)

THIN TILES - OPEN

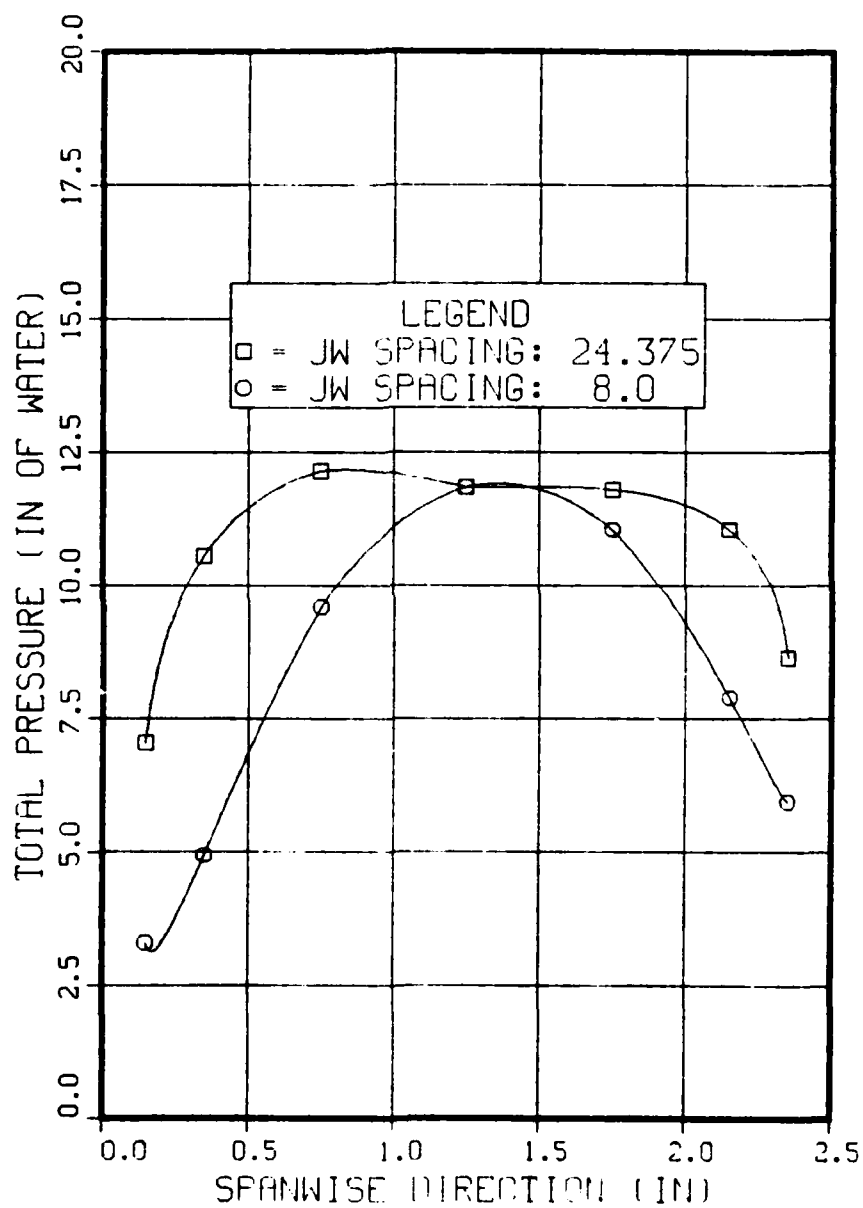


FIGURE 21

THROTTLING EFFECT IN FLOW ANGLE (WEST)

JW SPACING = 24.375 IN

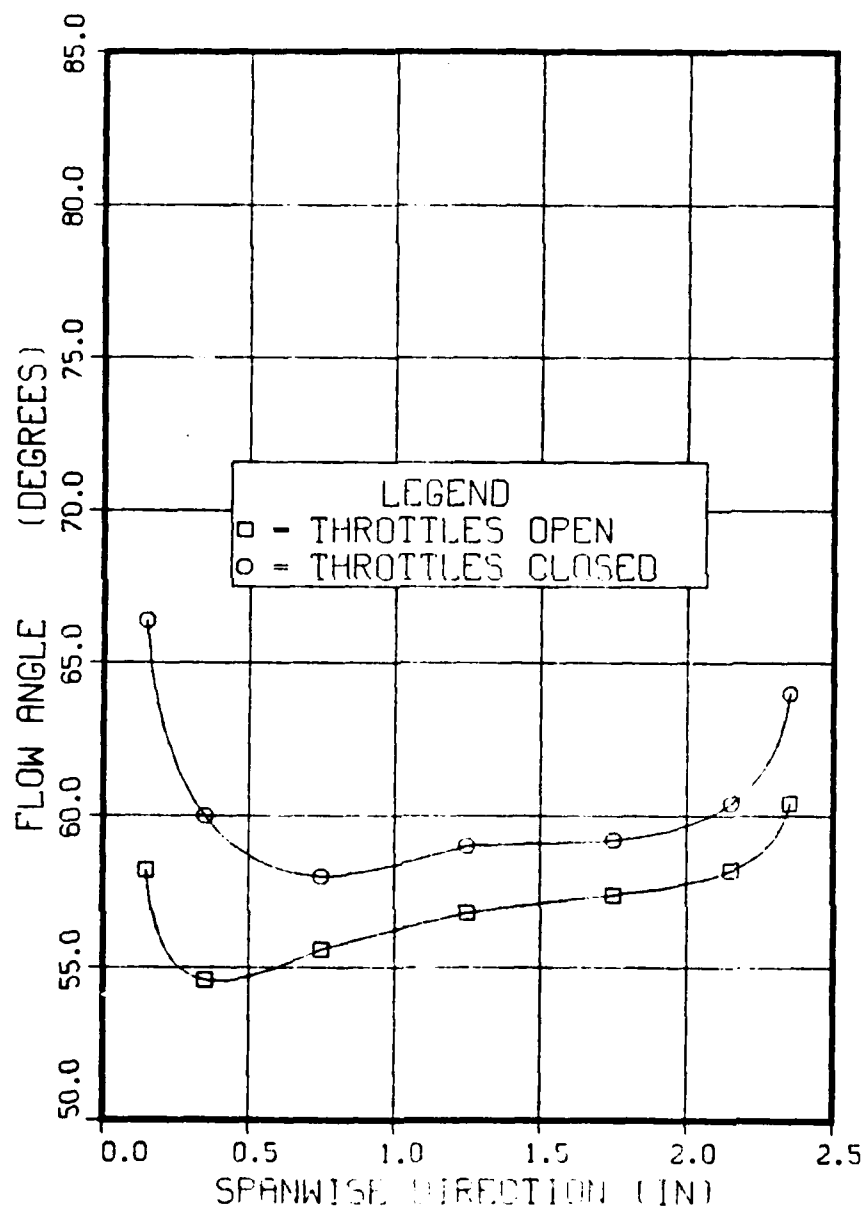


FIGURE 22

THROTTLING EFFECT IN FLOW ANGLE (WEST)

JW SPRING : 8.0 IN

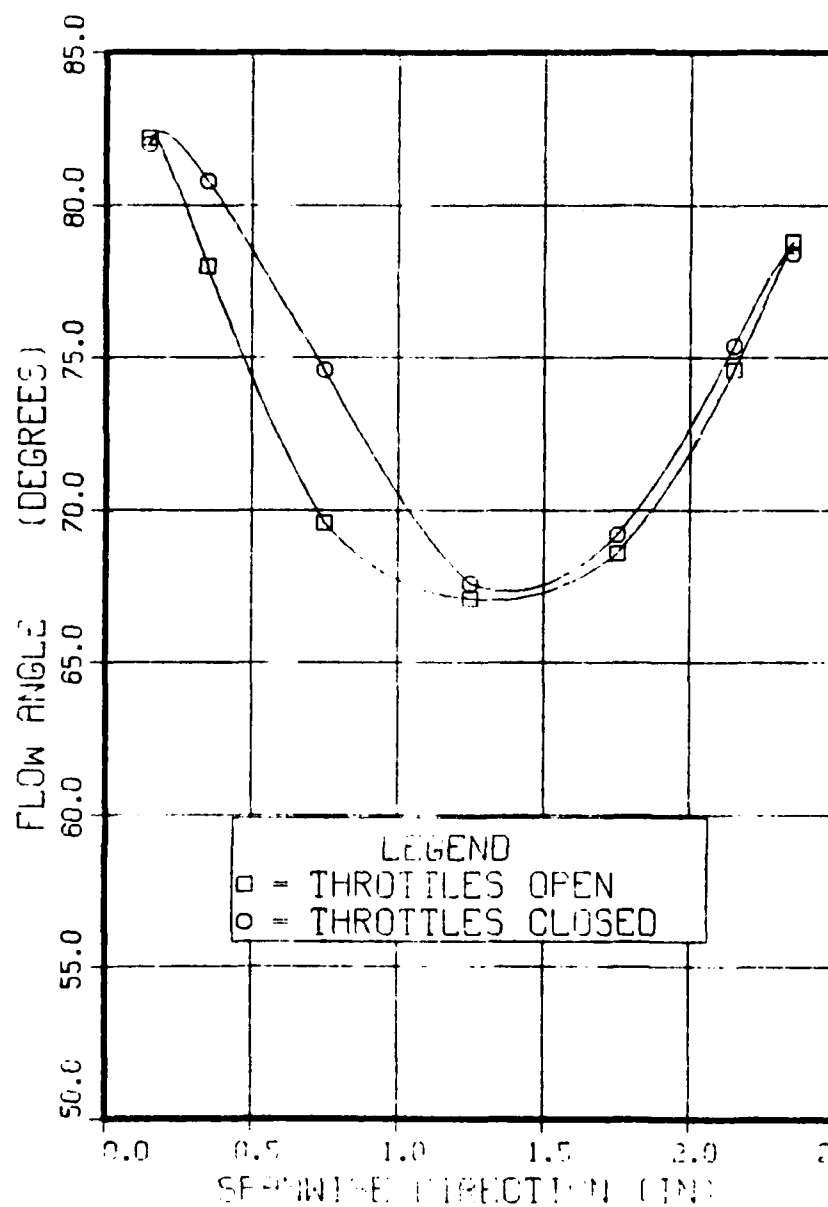


FIGURE 23

THROTTLING EFFECT IN TOTAL PRESSURE (WEST)

DOWN SPRING : 24.375 IN

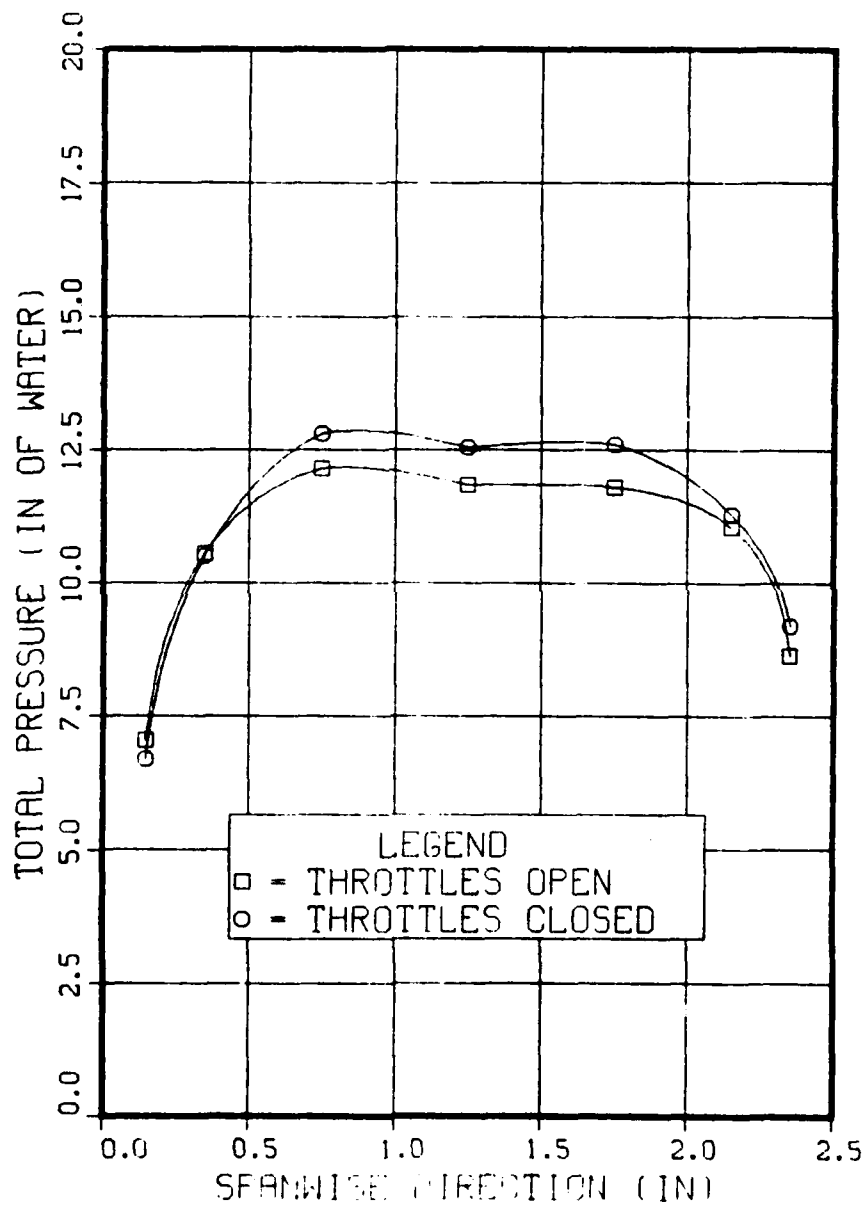
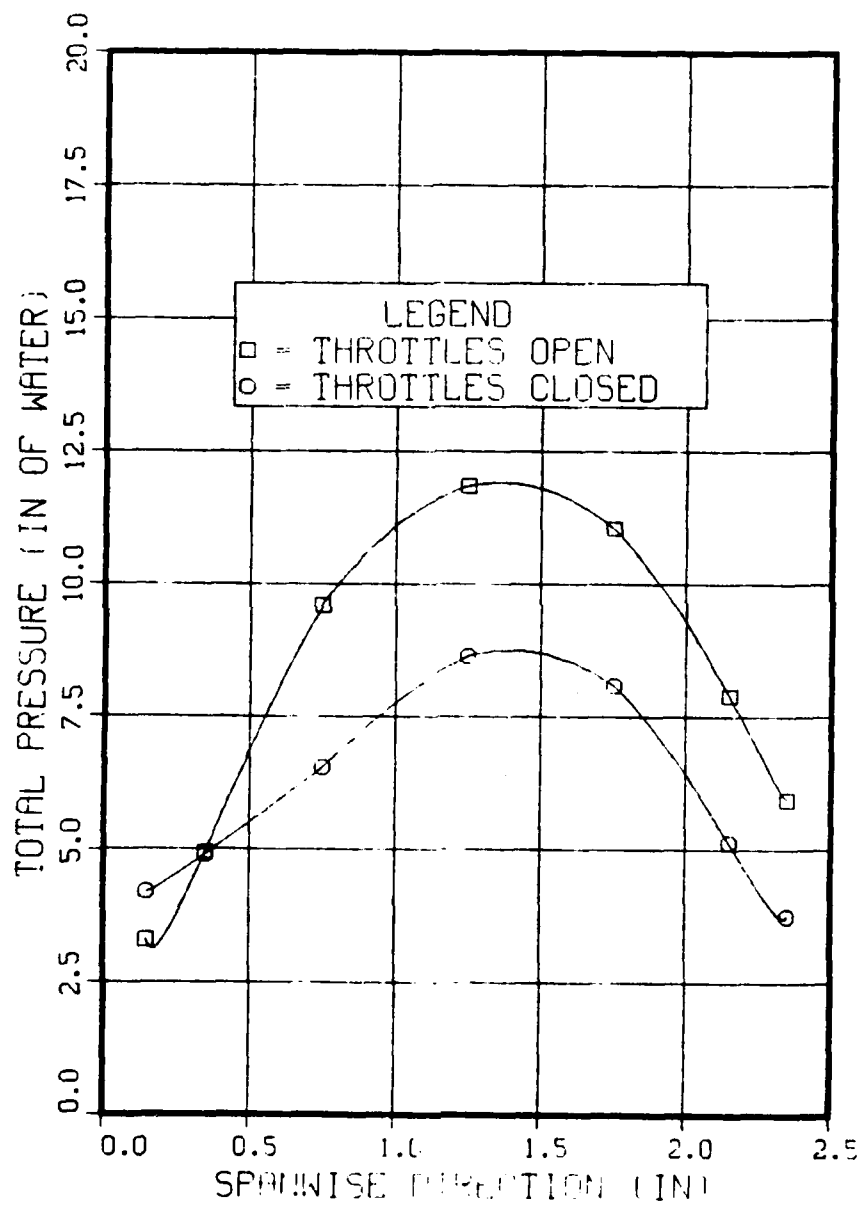




FIGURE 24

THROTTLING EFFECT ON TOTAL PRESSURE (WEST)

WIND SPEEDING : 8.0 IN



# FIGURE 25

CIRCUMFERENTIAL MEASUREMENTS (FLOW ANGLE)

W SPRING = 14.075 IN, THROTTLE = OPEN

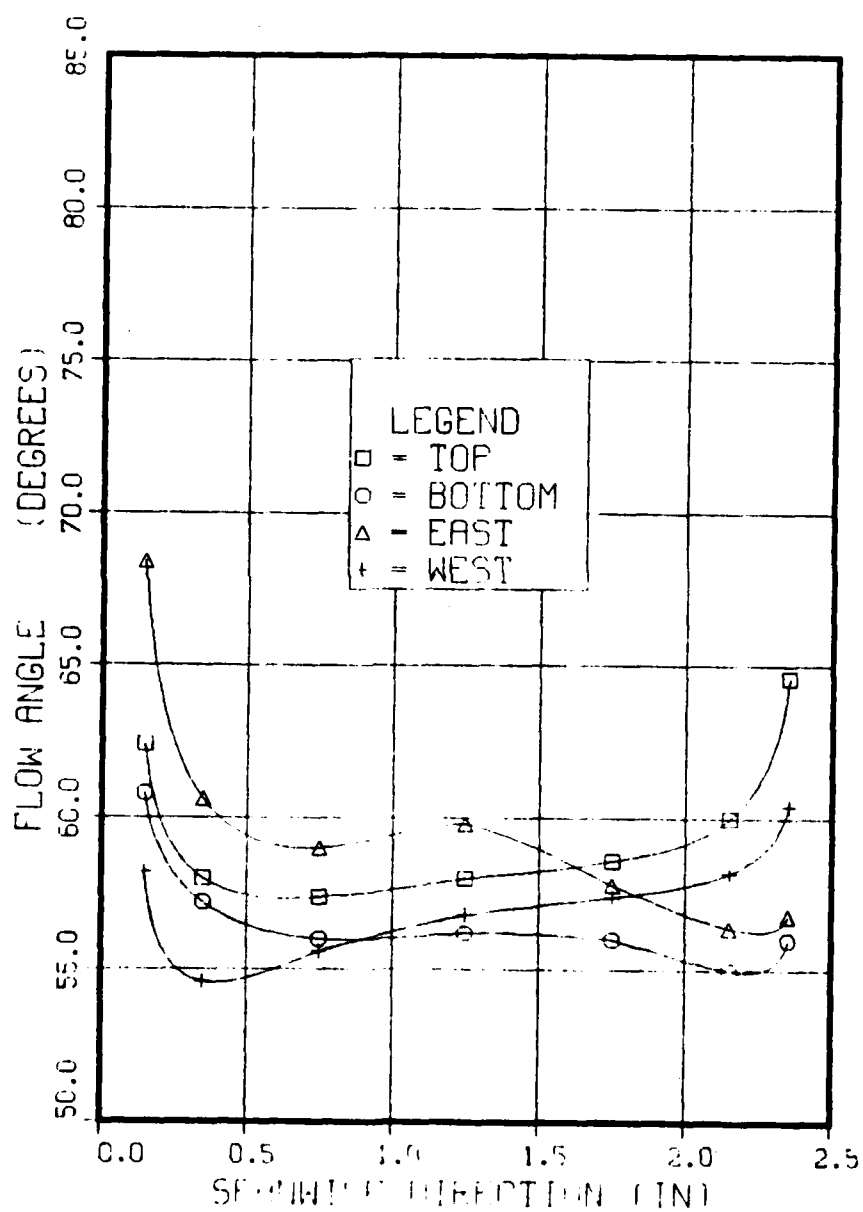


FIGURE 26

CIRCUMFERENTIAL MEASUREMENTS (FLOW ANGLE)

JW SPACING : 24.375 IN, THROTTLES : CLOSED

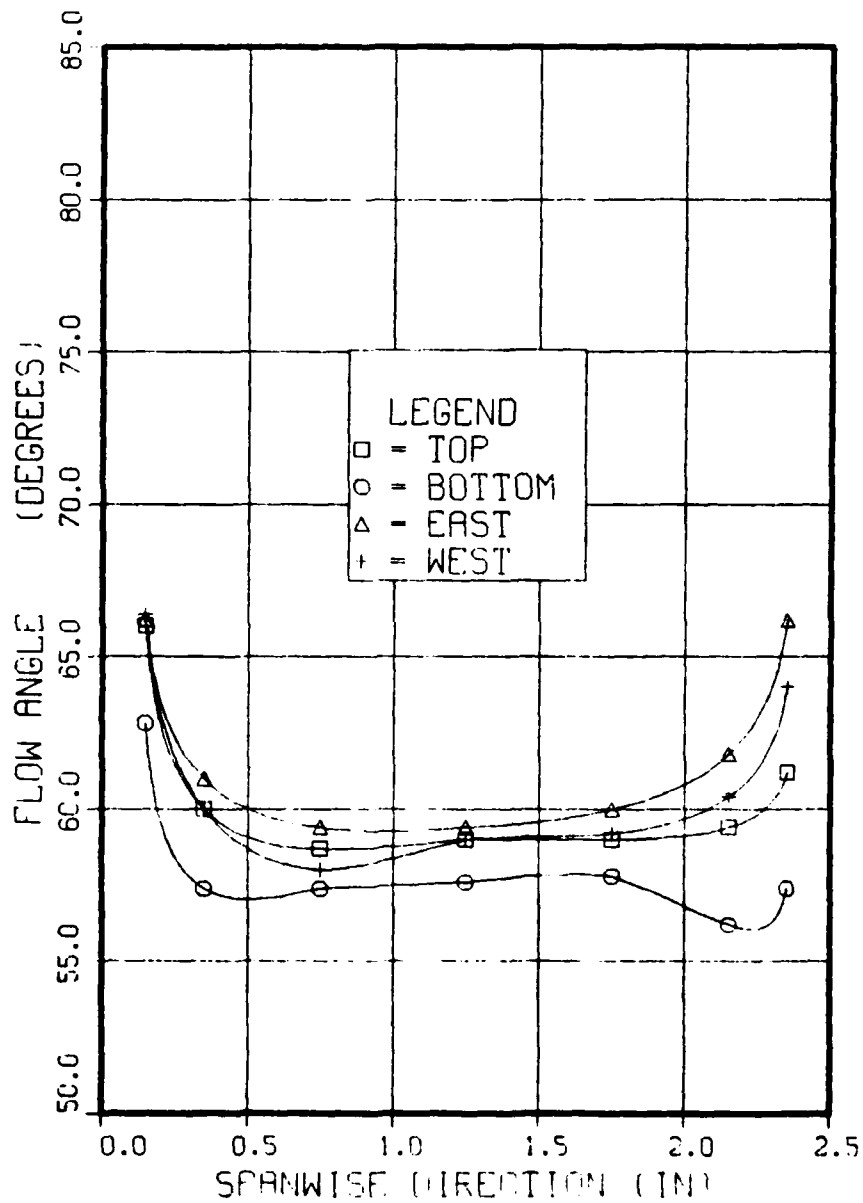


FIGURE 27

CIRCUMFERENTIAL MEASUREMENTS (PRESSURE)

W SPACING : 24.375 IN , THROTTLES : OPEN

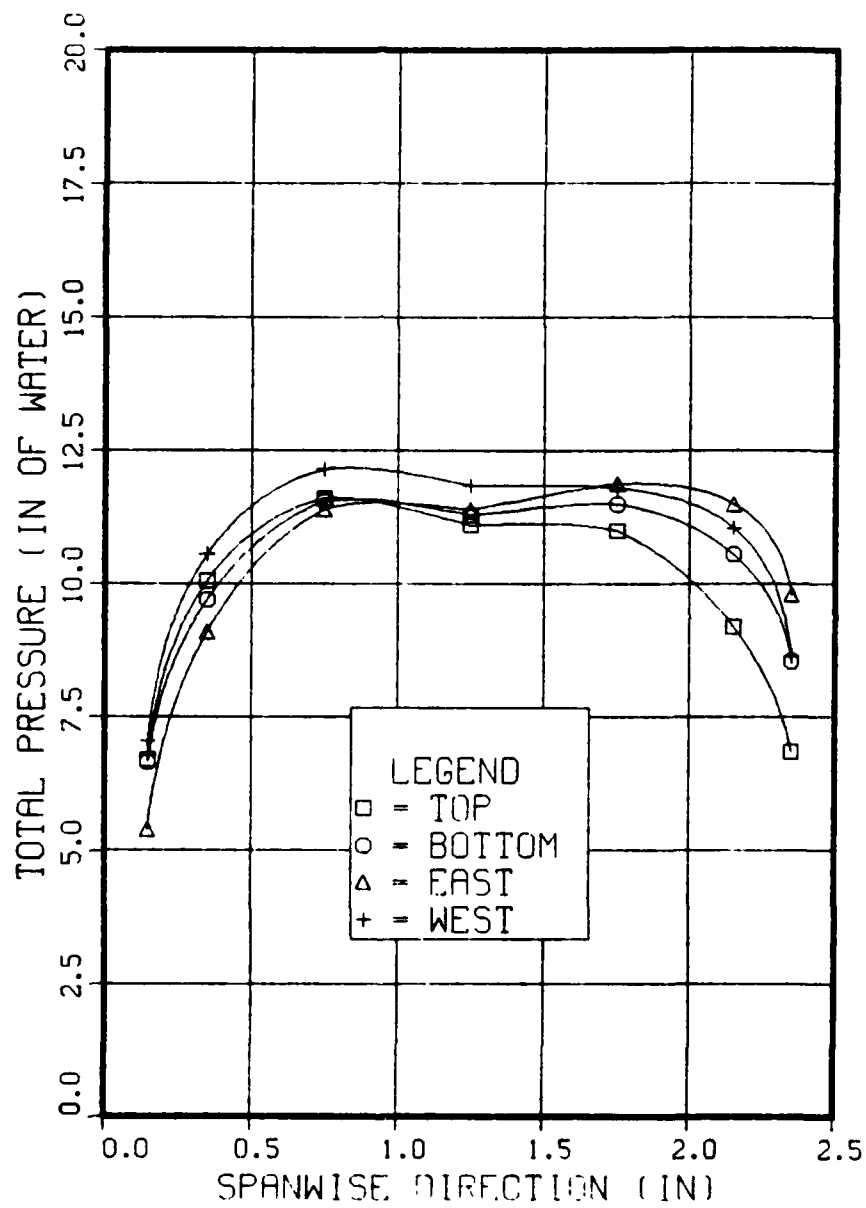


FIGURE 28

CIRCUMFERENTIAL MEASUREMENT (PRESSURE)

IN SPACING : 24.375 IN , THROTTLE : CLOSED

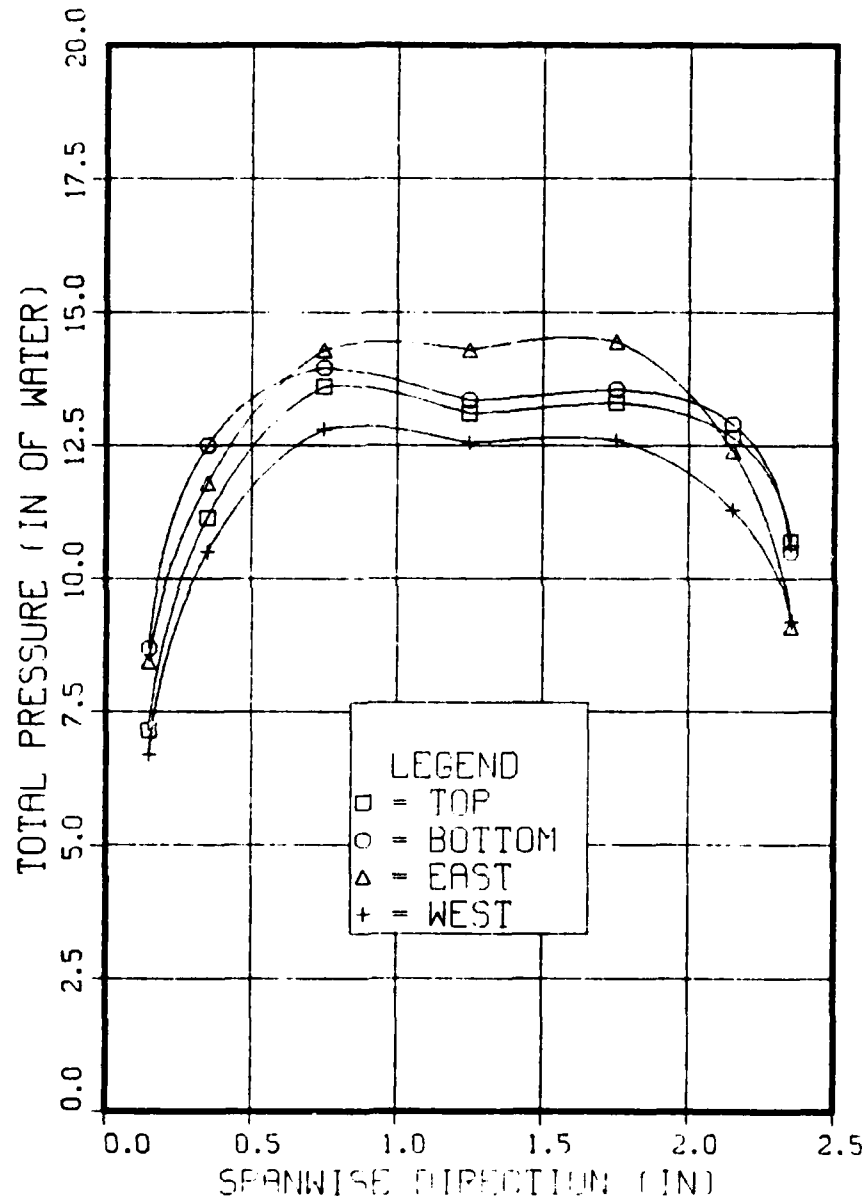
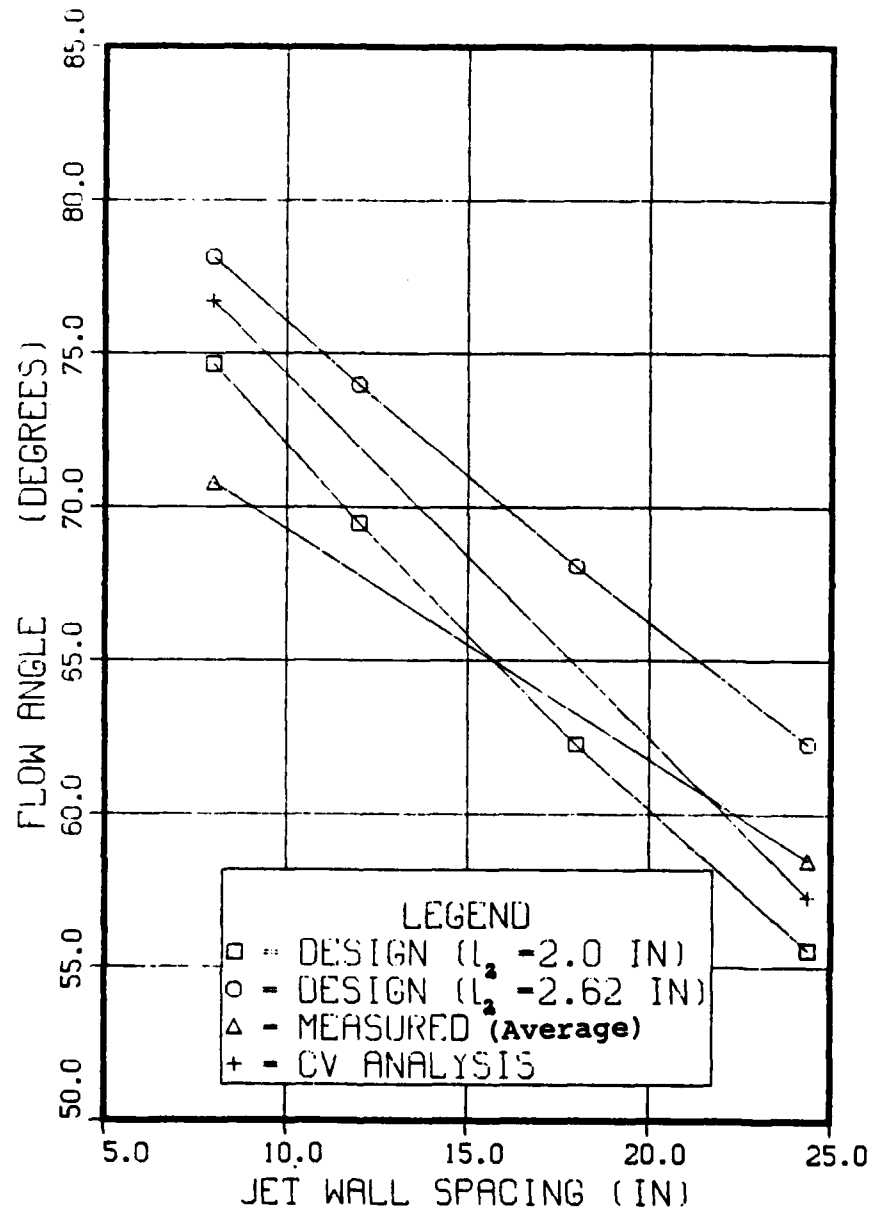


FIGURE 29

COMBINED PLOT OF MEASURED  
AND CALCULATED FLOW ANGLES.



APPENDIX A  
CDTD DESIGN CALCULATIONS

Assumptions:

1. The velocity coming out of the JW is the same as at the GC surface (Fig. A1).
2. No losses.
3. Constant density (incompressible) flow.

The velocity components are given by:

$$V_{R_i} = V_i \cos \beta_i \quad A(1)$$

and

$$V_{\theta_i} = V_i \sin \beta_i \quad A(2)$$

applying continuity between stations 1 and 2 (Fig. A1).

$$V_{\theta_1} \cdot Z \cdot A_{SV} \cdot N \cdot L_1 + V_{\theta_1} \cdot A_{JW} = V_{R_2} \cdot R_2 (2\pi L_2)$$

so that

$$L_1 = \frac{V_{R_2} R_2 (2\pi L_2) - V_{\theta_1} A_{JW}}{V_{\theta_1} Z A_{SV} N} \quad A(3)$$

Applying conservation of angular momentum:

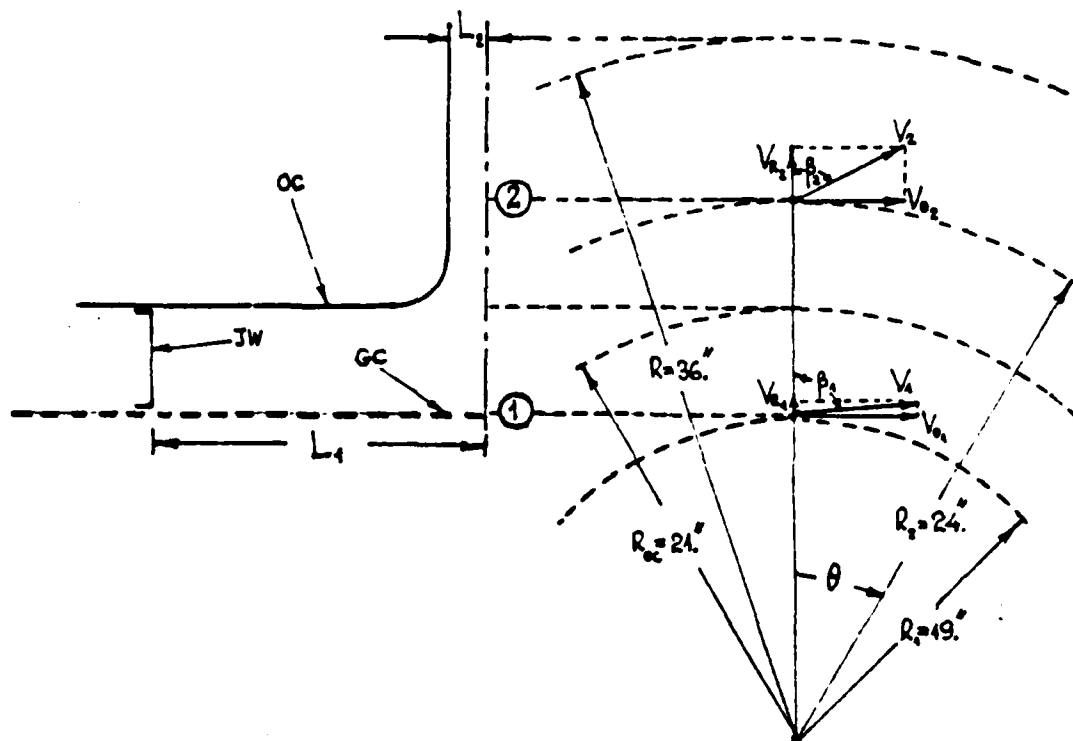


Figure A1. CDTD Schematic for the Design Calculations

$$V_{\theta_1} R_1 = V_{\theta_2} R_2 \quad A(4)$$

or

$$V_{\theta_1} = V_{\theta_2} \frac{R_2}{R_1} \quad A(4.1)$$

and substituting in A(3) for  $V_{\theta_1}$  from Eq. A(4.1)

$$L_1 = \left\{ \frac{R_1 (2\pi L_2)}{Z A_{SV} N} \right\} \frac{V_{R_2}}{V_{\theta_2}} - \frac{A_{JW}}{Z A_{SV} N} \quad A(5)$$



Substituting into Eq. A(5) the values for  $R_1$ ,  $L_2$ ,  $Z$ ,  $A_{SV}$ ,  $N$ , and  $A_{JW}$ , a linear relation is established between  $L_1$  and  $\cot \beta_2$ ; thus

$$L_1 = 25.97 \cot \beta_2 - 1.458 \quad A(6)$$

where data have been used for the as-manufactured test section span ( $l_2 = 2.61$ " ) and the short plywood walls.

For the designed span ( $l_2^* = 2$ " ), and plexiglass walls installed:

$$L_1^* = 19.9 \cot \beta_2 - 1.458 \quad A(7)$$

Equations A(6) and A(7) can also be solved for  $\beta_2$  and  $\beta_2^*$ ; thus

$$\beta_2 = \cot^{-1}(.0385L_1 + .056) \quad A(8)$$

$$\beta_2 = \cot^{-1}(.05025L_1^* + .07326) \quad A(9)$$

Using Equations A(8) and A(9) the following Table A1 is obtained:

TABLE A1  
 FLOW ANGLES ( $\beta_2$ ) AND CORRESPONDING  
 JW SPACING OBTAINED FROM EQUATIONS  
 A(8) AND A(9)

$\beta_2$	$\ell_1$ (in)	$\beta_2^*$	$\ell_1^*$ (in)
65.	21.304	65	15.643
70.	15.989	70	11.57
75.	11.001	75	7.748
62.29	24.375	55.56	24.375
68.075	18.00	62.27	18.00
73.987	12.00	69.456	12.00
78.14	8.00	74.663	8.00
79.2	7.00	76.01	7.00

## APPENDIX B

### FLOW MODELING CALCULATIONS FOR MERIDL INPUT

#### Assumptions:

1. Free vortex flow:  $V_{R_i} = \text{constant}$  (from hub to tip at a certain station) and  $V_z = \text{constant}$  with radius at constant  $z$ .
2. Constant density  $\rho = .076 \text{ LB}_m/\text{FT}^3$ .
3. Total velocity at the inlet of the TS,  $V_2 = 200 \text{ FPS}$
4. Axisymmetric flow.
5. Flow enters from Station 1-1 (Fig. 4) with constant whirl.

#### Flow Area at TS Inlet

$$A_2 = 2\pi R_2 L_2 = 1.3666 \text{ FT}^2$$

$$V_{R_2} = V_2 \cos \beta_2 = 200 \cos \beta_2 \text{ FPS}$$

$$\dot{m}_2 = \rho V_{R_2} A_2 = 20.772 \cos \beta_2 \text{ Lbm} \cdot \text{sec}^{-1}$$

#### Flow Area at Inlet (Station 1-1)

$$A_{IN} = \pi(R_S^2 - R_H^2) = 3.316 \text{ FT}^2$$

$$V_z = \text{constant}$$

Applying continuity between Station 1-1 and at the inlet of the test section:

$$\dot{m} = \rho_1 V_Z A_{IN} = \rho_2 V_{R_2} A_2 \quad B(1)$$

so that

$$V_Z = V_{R_2} \frac{A_2}{A_{IN}} = .412 V_{R_2} \quad B(2)$$

Free vortex flow implies that

$$V_{\theta_1} R_1 = V_{\theta_2} R_2 \quad B(3)$$

and solving for  $V_{\theta_1}$  and inserting values for  $R_1$  and  $R_2$ ,

$$V_{\theta_1} = 1.263 V_{\theta_2} \quad B(3.1)$$

Also,

$$V_{\theta_2} = V_2 \sin \beta_2 = 200 \sin \beta_2 \text{ (ft/sec)} \quad B(4)$$

For selected values of  $\beta_2$  the following Table B1 was constructed, using the above equations to obtain the corresponding whirl ( $R_1 V_{\theta_1}$ ) and the mass flow rate ( $\dot{m}$ ), required as input to MERIDL.

TABLE B1  
CALCULATED INPUT PARAMETERS FOR MERIDL CODE

$\beta_2$ (Deg)	$V_{R_2}$ (Ft/Sec)	$\dot{m}$ (lbs/Sec)	$V_{\theta_2}$ (Ft/Sec)	$V_{\theta_2} R_2$ (Ft <sup>2</sup> /Sec)
60	100	.3225	173.21	346.4
65	84.52	.2726	181.26	362.5
70	68.4	.2206	187.94	375.9
75	51.76	.167	193.19	386.4

## APPENDIX C

### CALCULATION OF THE MASS AVERAGED FLOW ANGLE

When the flow is non-uniform at the measurement plane, average values can be defined using the conservation equations. For example, applying conservation of angular momentum between the flow entering through the swirl vanes and the test section inlet:

$$\int_{\dot{m}_1} r_1 V_1 \sin \beta_1 d\dot{m}_1 - \int_{\dot{m}_2} r_2 V_2 \sin \beta_2 d\dot{m}_2 = r_1 \bar{V}_{\theta_1} \dot{m}_1 - r_2 \bar{V}_{\theta_2} \dot{m}_2 \quad C(1)$$

where  $\bar{V}_{\theta}$  is the mass flow average of the tangential velocity component which is defined as:

$$\bar{V}_{\theta} = \frac{1}{\dot{m}} \int_{\dot{m}} V_{\theta} d\dot{m} \quad C(2)$$

Similarly conservation of mass gives:

$$\begin{aligned} \dot{m} &= \int_0^{\ell} \rho_2 V_2 \cos \beta_2 (2\pi R_2) d\ell_2 = \int_0^{\ell} \rho_2 (2\pi R_2) V_{R_2} d\ell_2 \\ &= \rho_2 (2\pi R_2) K_{B_2} \bar{V}_{R_2} \ell_2 \quad C(3) \end{aligned}$$

where  $K_{B_2}$  is defined as the "blockage factor" and relates the area average ( $\bar{V}_{R_2}$ ) and mass average ( $\bar{V}_{R_2}$ ) velocity components, thus

$$K_{B_2} = \bar{V}_{R_2} / \bar{\bar{V}}_{R_2} \quad C(4)$$

Consistent with Eq. C(3) and Eq. C(4) the definition of the area-averaged radial component of velocity is:

$$\bar{V}_{R_2} = \frac{1}{\ell_2} \int_0^{\ell_2} V_{R_2} d\ell \quad C(5)$$

The mass-averaged radial component of velocity is obtained from Eq. E(3), thus

$$\bar{\bar{V}}_{R_2} = \frac{\dot{m}}{\rho_2 (2\pi R_2) K_{B_2} \ell_2} \quad C(6)$$

The mass-averaged flow angle ( $\bar{\bar{\beta}}_2$ ) can be defined from:

$$\tan \bar{\bar{\beta}}_2 = \frac{\bar{\bar{V}}_{\theta_2}}{\bar{\bar{V}}_{R_2}} \quad C(7)$$

so that

$$\bar{\bar{\beta}}_2 = \tan^{-1} \left( \frac{\bar{\bar{V}}_{\theta_2}}{\bar{\bar{V}}_{R_2}} \right) \quad C(8)$$

To obtain the value of  $\bar{\bar{\beta}}_2$ , from probe survey measurements, and blockage factor to use in the control volume analysis (Appendix D), the following data reduction is required:

1. Calculate the area-averaged radial velocity ( $\bar{V}_{R_2}$ ).

$$\bar{V}_{R_2} = \frac{1}{\ell_2} \int_{\ell} V_{R_2} d\ell = \frac{1}{\ell_2} \int_{\ell} V_2 \cos \beta_2 d\ell \quad C(9)$$

where, if the flow is assumed to be incompressible

$$V_2 = \left[ \frac{(P_1 - P_A)}{\rho/2} \right]^{.5} \quad C(10)$$

Substituting Eq. C(10) into C(9):

$$\bar{V}_{R_2} = \frac{1}{\ell_2} \left( \frac{2}{\rho} \right)^{.5} \int_{\ell_2} (P_1 - P_A)^{.5} \cos \beta_2 d\ell \quad C(11)$$

where  $\beta_2 \equiv \beta_2(\ell)$  is the measured flow angle at the exit of the plywood walls, and  $(P_1 - P_A)$  is the difference between the total pressure measured by the 5-hole probe and ambient.

2. Calculate the mass-averaged radial velocity using:

$$\bar{\bar{V}}_{R_2} = \frac{1}{\dot{m}} \int_{\dot{m}} V_{R_2} d\dot{m} = \frac{1}{\bar{V}_{R_2} \ell_2} \int_0^{\ell_2} V_{R_2}^2 d\ell \quad C(12)$$

3. Calculate the blockage factor using:

$$K_{B_2} = \frac{\bar{V}_{R_2}}{\bar{\bar{V}}_{R_2}} \quad C(13)$$



4. Calculate the mass-averaged tangential velocity using:

$$\bar{v}_{\theta_2} = \frac{1}{\dot{m}} \int_{\dot{m}} v_{\theta_2} d\dot{m} = \frac{1}{\bar{v}_{R_2} l_2} \int_0^{l_2} v_{\theta_2} v_{R_2} dl \quad C(14)$$

5. Calculate  $\bar{\beta}_2$  using Eq. C(8).

APPENDIX D  
CONTROL VOLUME ANALYSIS

1. The equation for  $\tan \beta_2$

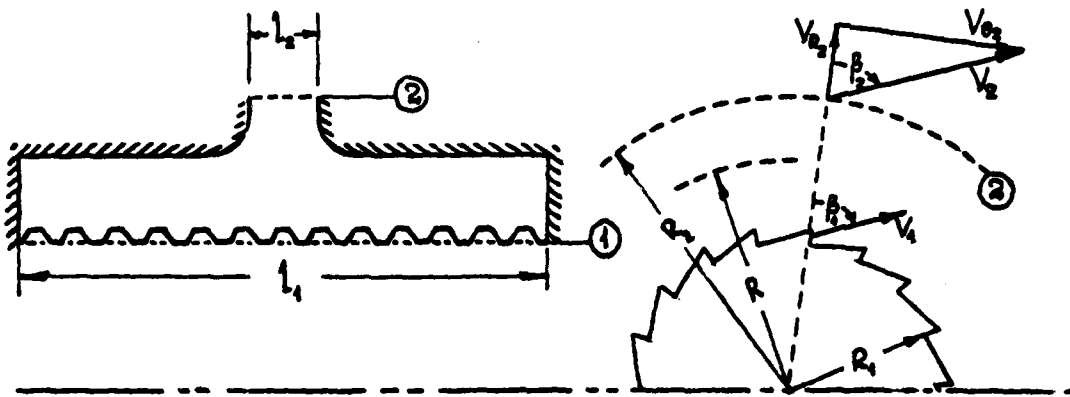


Figure D1. Control Volume Analysis Schematic

Assumptions:

1. Constant density  $\rho_1 = \rho_2$
2. Radial inlet surface  $S_1$  made up of small nozzles distributed along the GC.
3. The wall surface (IW) consists of:
  - a. The outside area of the GC;
  - b. The area of the JW faces;

c. Inside area of outer casing up to the test section inlet.

4. Uniform outlet conditions (Station 2).

5. Zero axial velocity ( $V_z$ ) at Stations 1 and 2.

Following Reference 6, the axial moment exerted by the air on the walls of the control volume (Fig. D1) is given by:

$$M_{aw} = \int_{S_1} \bar{R}_1 V_1 \sin \beta_1 \dot{dm}_1 - \int_{S_2} R_2 V_2 \sin \beta_2 \dot{dm}_2 + \int_{S_1} \vec{R}_1 \times d\vec{F}_1 + \int_{S_2} \vec{R}_2 \times d\vec{F}_2 \quad D(1)$$

The force on a surface element can be written in terms of its components normal to and in the surface as:

$$d\vec{F} = - p \hat{n} dS - \tau \hat{t} dS \quad D(2)$$

so that

$$\begin{aligned} \int_{S_1} \vec{R}_1 \times d\vec{F}_1 &= \int_{S_1} \vec{R}_1 \times (p_1 \hat{n} dS) \\ &= \bar{R}_1 p_1 A_1 N \ell_1 z \end{aligned} \quad D(3)$$

From continuity

$$\dot{m} = \int_{S_1} \dot{dm}_1 = \int_{S_2} \dot{dm}_2 \quad D(4)$$

so that

$$\int_{S_1} \dot{dm}_1 = \rho_1 V_1 \sin \beta_1 k_{B_1} A_1 Z N \ell_1 \quad D(4.1)$$

and

$$\int_{S_2} \dot{dm}_2 = \rho_2 V_2 \cos \beta_2 k_{B_2} (2\pi R_2) \ell_2 \quad D(4.2)$$

Substituting Eq. D(3), D(4.1) and D(4.2) into D(1):

$$\begin{aligned} M_{aw} = & \rho_1 \bar{R}_1 V_1^2 \sin^2 \beta_1 k_{B_1} A_1 Z N \ell_1 + \bar{R}_1 p_1 A_1 Z N \ell_1 \\ & - \rho_2 R_2 V_2^2 \sin \beta_2 \cos \beta_2 k_{B_2} (2\pi R_2) \ell_2 \end{aligned} \quad D(5)$$

The different terms in the LHS of Equation D(5), can be written in terms of the moments of the normal and tangential stress components given in Equation D(2). The only contributions to the axial moment, comes from shear stress components ( $\tau$ ) on the cylindrical walls, and normal stress components ( $p_w$ ) on the non cylindrical surfaces of the swirl vanes.

Thus:

$$M_{aw} = \int_{IW} \tau R dS + \int_a^b p_w R \sin \theta dS' \quad D(6)$$

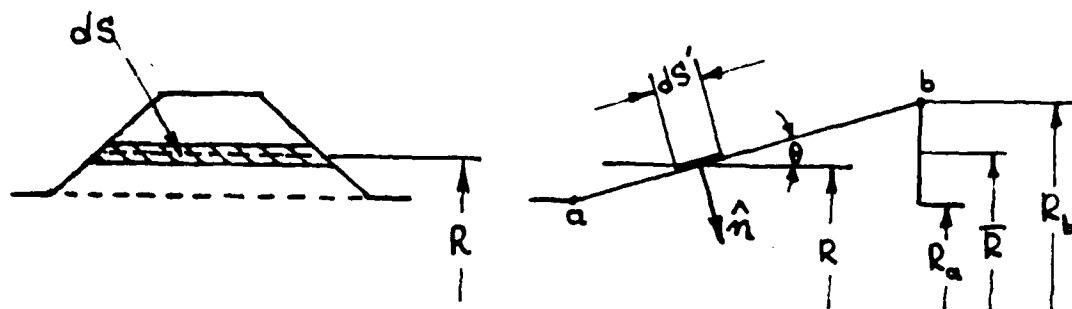


Figure D2. Stress Components on the Swirl Vanes

From Figure D2,

$$dS = dS' \sin \theta \quad D(7)$$

so that

$$M_{aw} = \int_{IW} \tau R dS + ZN\ell_1 \int_a^b p_w R dS \quad D(8)$$

Combining Equations D(5) and D(8)

$$\int_{IW} \tau R dS + ZN\ell_1 \int_a^b (p_w - p_1) R dS = \dot{m}(\bar{R}_1 V_1 \sin \beta_1 - R_2 V_2 \sin \beta_2) \quad D(9)$$

Solving Equation D(9) for  $\sin \beta_2$ , dividing both sides by  $\cos \beta_2$ , and substituting  $V_1$  and  $V_2$  from Equations D(4.1) and D(4.1), we obtain:

$$\tan \beta_2 = \frac{\bar{R}_1}{R_2} \times \left[ \frac{K_{B_2} (2\pi R_2)}{K_{B_1} A_{SV}} \right] \times \left\{ \frac{l_2}{l_1} \right\} \times \{1 - C_p - C_\tau\} \quad D(10)$$

where, the pressure term

$$C_p = \frac{ZNl_1}{\dot{m}V_1 \sin \beta_1} \int_a^b (p_w - p_1) \frac{R}{\bar{R}_1} ds \quad D(11)$$

and the friction term

$$C_\tau = \frac{1}{\dot{m}V_1 \sin \beta_1} \int_{IW} \tau \frac{R}{\bar{R}_1} ds \quad D(12)$$

The design analysis in Appendix A is the special case of  $C_p = C_\tau = 0$ . The values of  $C_p$  and  $C_\tau$  can be obtained using various assumptions.

## 2. Calculation of the Pressure Term

Writing,

$$\int_a^b \frac{R}{\bar{R}_1} ds \approx A_{SV} K_{B_1}$$

and  $(p_w - p_1) \neq f(R)$ , then

$$C_p \approx \frac{ZNl_1 A_{SV} K_{B_1}}{\dot{m}V_1 \sin \beta_1} (p_w - p_1) \quad D(13)$$

where  $(p_w - p_1)$  has a maximum value of  $(p_{t_1} - p_1)$ , or more realistically,  $(p'_{t_1} - p_1)$ , where  $p'_{t_1}$  is the stagnation pressure after jet mixing.

In order to calculate  $p'_{t1}$ , a sudden expansion is assumed downstream the swirl vanes. The following formula, derived in Reference 4, results from mixing at constant pressure:

$$\frac{p_w - p_1}{\frac{1}{2} \rho_1 V_1^2} = 2 \frac{A_1}{A_{MIX}} \left(1 - \frac{A_1}{A_{MIX}}\right) \quad D(14)$$

where  $A_{MIX}$  is the area of the flow when total mixing has occurred and the velocity is uniform.

From experimental measurements (Fig. D3), it was estimated that total mixing occurs within .3" from the GC surface, so as shown in Fig. D4 the area ratio is given by:

$$A_1/A_{MIX} = .3916$$

hence Equation D(14) becomes

$$p_w - p_1 = \frac{1}{2} \rho V_1^2 \times (.4765) \quad D(15)$$

Substituting to Equation D(13), the pressure term becomes:

$$C_p = \frac{(.23875)}{\sin^2 \beta_1} \quad D(16)$$

It is noted that the pressure term changes the value of  $\tan \beta_2$  by nearly 25%.

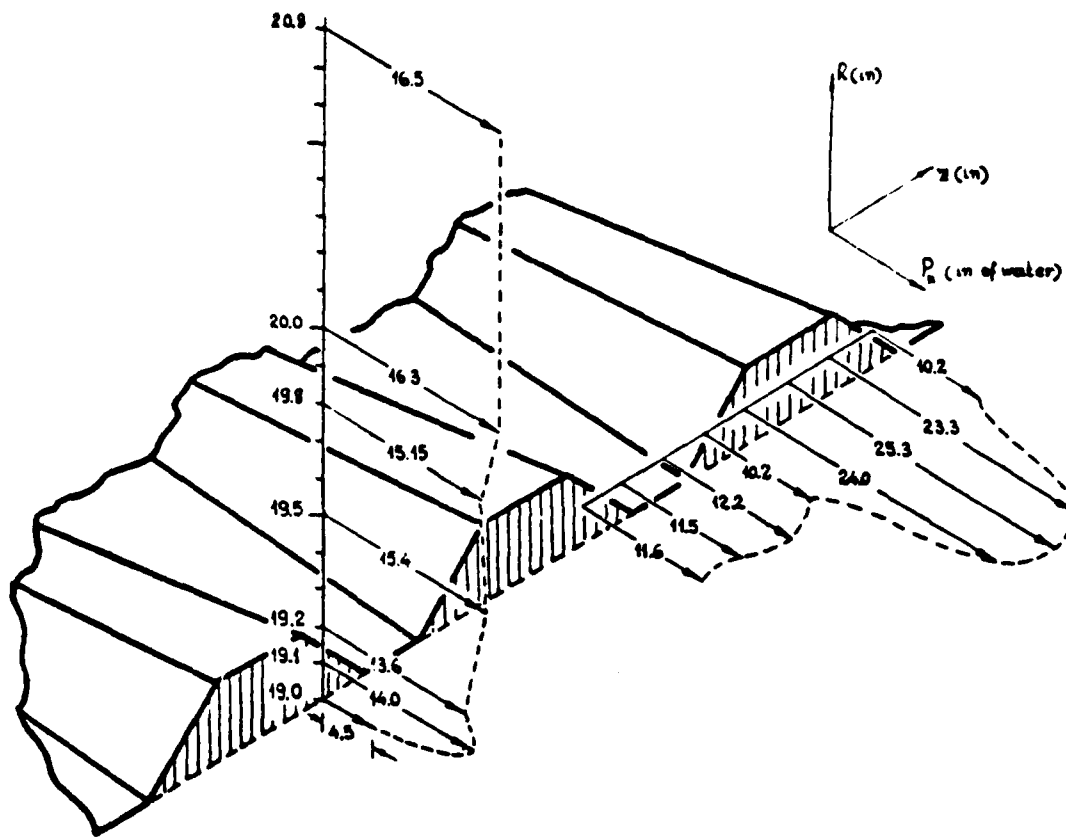


Figure D3. Total Pressure Distribution in the Flow Generator and Near the Surface of the Generating Cylinder Measured with a Kiel Probe

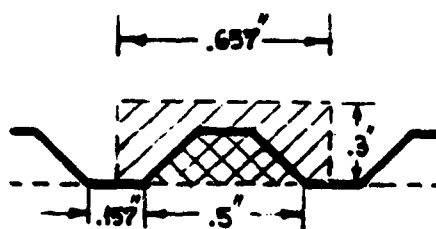


Figure D4.  $A_1/A_{MIX}$  Area Ratio Schematic



### 3. Calculation of the Friction Term

The friction term is approximated using an average velocity ( $\bar{V}_{IW}$ ) for the flow over the inner walls of the CDTD; the tangential stress is given by:

$$\tau = \frac{1}{2} C_F \rho \bar{V}_{IW}^2 \quad D(17)$$

and values are required for  $\bar{V}_{IW}$  and  $C_F$ .

#### a. Calculation of $\bar{V}_{IW}$

In terms of Kiel probe measurements,

$$V_1 = \left[ \frac{P_K - P_A}{\rho/2} (5.202) \right]^{.5} \quad D(18)$$

From Fig. D3 and using Eq. D(18) with the pressure differences ( $p_K - p_A$ ) from measurements and  $\rho = .002766$  <slugs/FT<sup>3</sup>>, the following Table D1 is obtained, for the velocity profile close to the surface of the GC.

Define the blockage factor for one jet as:

$$K_{B1} = \frac{\int_5^9 V_1(z) dz}{(z_9 - z_5) V_{1MAX}} = .841 \quad D(19)$$

where the average inlet velocity is given by

$$\bar{V}_1 = V_{1MAX} \times K_{B1} = 183.45 \text{ ft/sec} \quad D(20)$$

TABLE D1

VELOCITY PROFILE CALCULATION AT THE  
SURFACE OF THE GENERATING CYLINDER

Point #	$2(p_K - p_A)$ (in $H_2O$ )	$V_1$ (FPS)
1	14.0	162.0
2	11.6	147.7
3	11.5	147.06
4	12.2	151.5
5	10.2	138.5
6	24.0	212.45
7	25.3	218.13
8	23.3	209.33
9	10.2	138.5

The velocity over the outer casing walls ( $V_{ow}$ ) can be approximated from the pressure difference to atmosphere measured at  $R = 20.8''$  (Fig. D4), then

$$V_{ow} = \left[ \frac{\Delta P (R = 20.8'')}{\rho/2} (5.202) \right]^{.5} = 176.16 \text{ FPS} \quad D(21)$$

From Equations D(20) and D(21) the average velocity over the inner walls ( $\bar{V}_{IW}$ ) can be estimated:

$$\bar{V}_{IW} = \frac{\bar{V}_1 + V_{ow}}{2} = 179.8 \text{ FPS} \quad D(22)$$

b. Calculation of  $C_F$

The hydraulic diameter [Ref. 5] is used to calculate the Reynolds number. The Reynolds number is given by:

$$Re = \frac{d_h \bar{V}_{IW}}{\nu} \quad D(23)$$

where

$$d_h = \frac{4A}{C} \quad D(24)$$

and A denotes the cross-sectional area and C the wetted perimeter.

For the CDTD

$$A = 2\ell_1 + 4\ell_2 \equiv .41 \text{ FT}^2$$

$$C = 2\ell_1 + 12 \equiv 5.0625 \text{ FT}$$

hence

$$d_h = .324 \text{ FT} \quad D(24.1)$$

For  $\nu = 1.57 \times 10^{-4} \text{ FT}^2/\text{sec}$ , Eq. D(23) gives:

$$Re = 3.63 \times 10^5 \quad D(25)$$

From Prandtl's universal law of friction for turbulent flows through pipes [Ref. 5]:

$$C_F = 3.59 \times 10^{-3} \quad D(26)$$

Substituting all specified terms into Eq. D(12):

$$C_T = \frac{1.795 \times 10^{-3}}{\sin^2 \beta_1} \times \left( \frac{A_{IW}}{A_{T1}} \right) \left( \frac{\bar{V}_{IW}}{\bar{V}_1} \right)^2 \quad D(27)$$

#### 4. Calculation of Outlet Angle

Using Eq. D(16) and Eq. D(27) in Eq. D(10),

$$\tan \beta_2 = \frac{\bar{R}_1}{R_2} \times \left( \frac{A_{T2}}{A_{T1}} \right) \left[ 1 - \frac{.23875}{\sin^2 \beta_1} - \frac{1.795 \times 10^{-3}}{\sin^2 \beta_1} \left( \frac{\bar{V}_{IW}}{\bar{V}_1} \right)^2 \left( \frac{A_{IW}}{A_{T1}} \right) \right] \quad D(28)$$

For the values:

$$\bar{R}_1 = 19.1 \text{ in}$$

$$R_2 = 25 \text{ in}$$

$$l_2 = 2.62 \text{ in}$$

$$A_{T1} = A_{SV} Z N l_1 k_{B1} = 5.045 l_1 \text{ in}$$

$$k_{B2} (l_1 = 24.375) = .925 \text{ (average measured)}$$

$$k_{B2} (l_1 = 8.0) = .83 \text{ (average measured)}$$

$$A_{T2} = 2\pi R_2 \ell_2 k_{B_2} = 411.55 k_{B_2} \text{ in}^2$$

$$\begin{aligned} A_{IW} &= 2\pi \bar{R}_1 \ell_1 + 2\pi R_{OC}(\ell_1 - \ell_2) + 2\pi(R_{OC}^2 - R_1^2) + 2\pi(R_2^2 - R_{OC}^2) \\ &= 7454 \text{ in}^2 \end{aligned}$$

$$\beta_1 = 84^\circ$$

Substituting these values into Eq. D(28), the flow angle as a function of the exposed length ( $\ell_1$ ) of the generating cylinder (since  $k_{B_2}$  is also a function of  $\ell_1$ ) is given by:

$$\beta_2 = \tan^{-1} \left[ (40.78) \left\{ \frac{k_{B_2}}{\ell_1} \right\} \right] \quad D(29)$$

From Eq. D(29), for  $\ell_1 = 24.375$ " and  $k_{B_2} = .925$ :

$$\beta_2 (\ell_1 = 24.375) = 57.13^\circ$$

Also, for  $\ell_1 = 8.0$  in and  $k_{B_2} = .83$ ; Eq. D(29) gives:

$$\beta_2 (\ell_1 = 8.0) = 76.7^\circ .$$

## MERIDL INPUT FILES

[illegible]

0100 15 05130 46414 112 - 1.335 101 12 - 03. 01/4/03

RESEARCH	INPUT	DATA	BY	TIME	MINIMUM	OF	UNICA	REFAC	YELTOL	FNEW
1-10-100	PAS	1710-100	21	1000				1-10000	1000000-01	500000
201	MC	1710-100	21	1000					YELTOL	
130	11	1710-100	21	1000					YELTOL	
45-100	ANAL	1710-100	21	1000					YELTOL	

[illegible][illegible][illegible][illegible]

DATE 15 JUL 1964 112 - 1.305 141 42 - 10. 0/4/03

[illegible][illegible]

UPSTREAM	INPUT	DATA	MIN	RTN	
5000000	ARRAY	1.416670	1.50000	1.625000	1.666670
1.416670	ARRAY	1.500000	1.51670	1.583340	1.666670
1.500000	ARRAY	1.583340	1.50000	1.51670	1.666670
1.583340	ARRAY	1.500000	1.51670	1.583340	1.666670
1.666670	ARRAY	1.500000	1.51670	1.583340	1.666670
1.750000	ARRAY	1.500000	1.51670	1.583340	1.666670
1.833330	ARRAY	1.500000	1.51670	1.583340	1.666670
1.916660	ARRAY	1.500000	1.51670	1.583340	1.666670
2.000000	ARRAY	1.500000	1.51670	1.583340	1.666670
2.083330	ARRAY	1.500000	1.51670	1.583340	1.666670
2.166660	ARRAY	1.500000	1.51670	1.583340	1.666670
2.250000	ARRAY	1.500000	1.51670	1.583340	1.666670
2.333330	ARRAY	1.500000	1.51670	1.583340	1.666670
2.416660	ARRAY	1.500000	1.51670	1.583340	1.666670
2.500000	ARRAY	1.500000	1.51670	1.583340	1.666670
2.583330	ARRAY	1.500000	1.51670	1.583340	1.666670
2.666660	ARRAY	1.500000	1.51670	1.583340	1.666670
2.750000	ARRAY	1.500000	1.51670	1.583340	1.666670
2.833330	ARRAY	1.500000	1.51670	1.583340	1.666670
2.916660	ARRAY	1.500000	1.51670	1.583340	1.666670
3.000000	ARRAY	1.500000	1.51670	1.583340	1.666670
3.083330	ARRAY	1.500000	1.51670	1.583340	1.666670
3.166660	ARRAY	1.500000	1.51670	1.583340	1.666670
3.250000	ARRAY	1.500000	1.51670	1.583340	1.666670
3.333330	ARRAY	1.500000	1.51670	1.583340	1.666670
3.416660	ARRAY	1.500000	1.51670	1.583340	1.666670
3.500000	ARRAY	1.500000	1.51670	1.583340	1.666670
3.583330	ARRAY	1.500000	1.51670	1.583340	1.666670
3.666660	ARRAY	1.500000	1.51670	1.583340	1.666670
3.750000	ARRAY	1.500000	1.51670	1.583340	1.666670
3.833330	ARRAY	1.500000	1.51670	1.583340	1.666670
3.916660	ARRAY	1.500000	1.51670	1.583340	1.666670
4.000000	ARRAY	1.500000	1.51670	1.583340	1.666670
4.083330	ARRAY	1.500000	1.51670	1.583340	1.666670
4.166660	ARRAY	1.500000	1.51670	1.583340	1.666670
4.250000	ARRAY	1.500000	1.51670	1.583340	1.666670
4.333330	ARRAY	1.500000	1.51670	1.583340	1.666670
4.416660	ARRAY	1.500000	1.51670	1.583340	1.666670
4.500000	ARRAY	1.500000	1.51670	1.583340	1.666670
4.583330	ARRAY	1.500000	1.51670	1.583340	1.666670
4.666660	ARRAY	1.500000	1.51670	1.583340	1.666670
4.750000	ARRAY	1.500000	1.51670	1.583340	1.666670
4.833330	ARRAY	1.500000	1.51670	1.583340	1.666670
4.916660	ARRAY	1.500000	1.51670	1.583340	1.666670
5.000000	ARRAY	1.500000	1.51670	1.583340	1.666670
5.083330	ARRAY	1.500000	1.51670	1.583340	1.666670
5.166660	ARRAY	1.500000	1.51670	1.583340	1.666670
5.250000	ARRAY	1.500000	1.51670	1.583340	1.666670
5.333330	ARRAY	1.500000	1.51670		

ECCHASISHEAM	INPUT	DATA	MMJUT	RTJUT	2.581330
2.225000	1.916670		2.474600		
2.225000	2.250000		2.520800	2.541700	2.562500
2.225000	2.555555	-03	.5999999E-03	.1999999E-03	.5999999E-03
2.225000	2.555555	-03	.5999999E-03	.1999999E-03	.5999999E-03

MULTIPLY INTEGRAL LINE PLCM FRAC TICAL DATA	
W PLCM AREA	
0.50000000-01	10000000
0.47500000	50000000
0.45000000	100000000
0.42500000	150000000
0.40000000	200000000
0.37500000	250000000
0.35000000	300000000
0.32500000	350000000
0.30000000	400000000
0.27500000	450000000
0.25000000	500000000
0.22500000	550000000
0.20000000	600000000
0.17500000	650000000
0.15000000	700000000
0.12500000	750000000
0.10000000	800000000
0.07500000	850000000
0.05000000	900000000
0.02500000	950000000
0.00000000	1000000000



CUTG 15 US1000 112 - 1.305 1A1 92 - 75. 0/7/81

[illegible][illegible][illegible]

## MERIDI OUTPUT FILES

FULL MASSFLUX  
TUNING  
ITERATION NO. 3

[illegible]

SUR.  
 PAL-  
 SUM.  
 SUC-  
 VAL-  
 STIRAY.  
 REL-FLOM  
 ANGLE  
 VERID-  
 ANGLE  
 CRITVEL-  
 RAJUL  
 TEL.  
 REL-LANG.  
 VERID-  
 VEL.  
 MENIU-  
 CUBU-  
 REVAL  
 ARAL.  
 CUBU-

AD-A136 874

FLOW GENERATION IN A NOVEL CENTRIFUGAL DIFFUSER TEST  
DEVICE(U) NAVAL POSTGRADUATE SCHOOL MONTEREY CA  
P VIDOS SEP 83

2/2

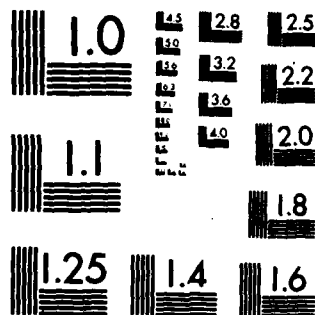
UNCLASSIFIED

F/G 20/4

NL



END  
DATE  
FILMED  
2-84  
DTIC



MICROCOPY RESOLUTION TEST CHART  
NATIONAL BUREAU OF STANDARDS-1963-A





[illegible][illegible]

FULL MASSFLUX  
 ILLATION NO. 2

```

000 STREAMLINE NUMBER | -- STRAP FUNCTION = 0.0 00

```

[illegible]

00 STREAMLINE NUMBER 2 --- STREAM FUNCTION = 0.0503 00

[illegible]



[illegible]

FULL MASSFLUX  
ITERATION NL. 2

```
000 STREAMLINE NUMBER ! -- STREAM FUNCTION = 0.0 00
```

[illegible]

-- ? 470981S 00 00

[illegible]



#### LIST OF REFERENCES

1. Erwin, John R., Development and Use of Centrifugal Diffuser Test Device, Naval Postgraduate School Turbopropulsion Laboratory Technical Proposal 81-006, 1981.
2. Katsanis, Theodore, and William D. McNally, Revised FORTRAN Program for Calculating Velocities and Streamlines on the Hub-Shroud Midchannel Stream Surface of an Axial, Radial or Mixed Flow Turbomachine or Annular Duct (User's Manual and Programmer's Manual), Lewis Research Center, Cleveland, Ohio, March 1977.
3. Shreeve, R.P., Calibration of Flow Nozzles Using Traversing Pitot-Static Probes, Naval Postgraduate School, Monterey, California, July 1973.
4. Zucker, Robert D., Fundamentals of Gas Dynamics, Naval Postgraduate School, Monterey, California, 1977.
5. Schlichting, Herman, Boundary Layer Theory, 7th Edition, 1979.
6. Vavra, M.H., Aero-Thermodynamics and Flow in Turbo-machines, 1974.

INITIAL DISTRIBUTION LIST

	No. Copies
1. Defense Technical Information Center Cameron Station Alexandria, Virginia 22314	2
2. Library, Code 0142 Naval Postgraduate School Monterey, California 93943	2
3. Department Chairman, Code 67 Department of Aeronautics Naval Postgraduate School Monterey, CA 93943	1
4. Dr. R.P. Shreeve, Code 67Sf Naval Postgraduate School Monterey, CA 93943	10
5. Mr. George Derderian Naval Air Systems Command Code AIR-310E Department of the Navy Washington, C.D. 20360	1
6. Dr. A.D. Wood Office of Naval Research 800 N. Quincy St. Arlington, VA 22217	1
7. Chief, Fan and Compressor Branch (Attn: Dr. J. Wood) NASA Lewis Research Center Mail Stop 5-9 21000 Brookpart Road Cleveland, OH 44135	2
8. Embassy of Greece Office of the Air Attache 2228 Massachusetts Avenue N.W. Washington, D.C. 20008	3
9. Captain (HAF) Vidos Panagiotis 165, Karaïskou St. Piraeus, Greece	2